UNIVERSITY *of* York

This is a repository copy of *A MAPK/c-Jun-mediated switch regulates the initial adaptive and cell death responses to mitochondrial damage in a neuronal cell model*.

White Rose Research Online URL for this paper:
https://eprints.whiterose.ac.uk/135930/

Version: Accepted Version

Article:

White Rose
university consortium
Universities of Leeds, Sheffield & York

eprints@whiterose.ac.uk
https://eprints.whiterose.ac.uk/

A MAPK/c-Jun-mediated switch regulates the initial adaptive and cell death responses to mitochondrial damage in a neuronal cell model

Thomas A. Ryan[1], Katherine M. Roper[1], Jacquelyn Bond[1], Sandra M. Bell[1], Sean T. Sweeney[2], Ewan E. Morrison[1]*

[1] Leeds Institute of Biological and Clinical Sciences, Wellcome Trust Brenner Building, St James University Hospital, University of Leeds, Leeds, West Yorkshire, LS9 7TF

[2] Department of Biology, University of York, Heslington, York, North Yorkshire, YO10 5DD

* Corresponding author
Email: e.e.morrison@leeds.ac.uk (EM)

Abstract

Parkinson's disease (PD) is defined by the progressive loss of dopaminergic neurons. Mitochondrial dysfunction and oxidative stress are associated with PD although it is not fully understood how neurons respond to these stresses. How adaptive and apoptotic neuronal stress response pathways are regulated and the thresholds at which they are activated remains ambiguous. Utilising SH-SY5Y neuroblastoma cells, we show that MAPK/AP-1 pathways are critical in regulating the response to mitochondrial uncoupling. Here we found the AP-1 transcription factor c-Jun can act in either a pro- or anti-apoptotic manner, depending on the level of stress. JNK-mediated cell death in differentiated cells only occurred once a threshold of stress was surpassed. We also identified a novel feedback loop between Parkin activity and the c-Jun response, suggesting defective mitophagy may initiate MAPK/c-Jun-mediated neuronal loss observed in PD. Our data supports the hypothesis that blocking cell death pathways upstream of c-Jun as a therapeutic target in PD may not be appropriate due to crossover of the pro- and anti-apoptotic responses. Boosting adaptive responses or targeting specific aspects of the neuronal death response may therefore represent more viable therapeutic strategies.

1. Introduction

Parkinson's disease (PD) is a neurodegenerative disorder characterised by the loss of dopaminergic neurons in the substantia nigra pars compacta (SNpc). Although oxidative stress and mitochondrial dysfunction are prominent

Parkinson's disease (PD) is a neurodegenerative disorder characterised by the loss of dopaminergic neurons in the substantia nigra pars compacta (SNpc). Although oxidative stress and mitochondrial dysfunction are prominent characteristics of familial and sporadic PD, the precise pathways driving pathological changes are yet to be fully defined.

A number of studies have implicated immediate early gene (IEG) signalling in PD ([1-9]). IEG proteins, such as Fos and Jun transcription factors, are regulators of the early stress response. Fos and Jun proteins dimerise to form activating protein-1 (AP-1) transcription factor complexes, which regulate the expression of genes containing the TPA responsive element (TRE) consensus sequence (5'-TGA(G/C)TCA-3') within their promoter ([10], [11]). Increased activity of the AP-1 transcription factor c-Jun, a downstream target of c-Jun amino N-terminal kinase (JNK), has been found in dopaminergic neurons of PD patients ([1]), although JNK inhibition in clinical trials has yet to yield positive results ([12]). AP-1 activity and stability can be rapidly modulated by phosphorylation in response to stimuli ([13]), with JNK, an AP-1 regulator, implicated in several neurodegenerative conditions ([14]).

The MAPK, extracellular signal-regulated kinase (ERK) can regulate the activity of JNK and c-Jun ([15], [16]), has been implicated in the mitochondrial stress response ([17], [18]) and regulates the neuronal response to different forms of L-DOPA-induced oxidative stress via c-Jun ([9]). With the complexity of crosstalk, coupled with signal-dependent thresholds, it seems probable that multiple pathways coordinate adaptive and apoptotic stress responses in neurons. Even specific stress response mechanisms can share common elements or be activated in parallel ([19]). Cells initiate protective or apoptotic responses depending on the level or duration of stress. The capacity of the initial response dictates the eventual outcome ([20]). In post-mitotic neurons, adaptive responses are critical since their failure will lead to progressive neurodegeneration.

Most intracellular reactive oxygen species (ROS) are produced by mitochondria ([21]). Excessive ROS associated with PD are produced by dysfunctional mitochondria, which undergo selective autophagy, a process called mitophagy ([22]). The *PARK2 (PARKIN)* and *PARK6* genes (encoding Parkin and PTEN-induced putative kinase 1 (PINK1), respectively) are linked to familial PD ([23]), with *PARKIN* mutations the most common cause of autosomal-recessive PD ([24], [25]). Upon mitochondrial depolarisation, PINK1 accumulates on the mitochondrial outer membrane (MOM), recruiting and activating the E3 ubiquitin ligase Parkin ([26-28]) to promote mitophagy ([29]). Excessive ROS activates the apoptosis signalling kinase 1 (ASK1)/JNK pathway ([30-33]). As Parkin activity can repress JNK/c-Jun activity ([4], [34]) and c-Jun represses *PARKIN* expression ([7]), a feedback loop may exist between multiple pathways to determine the response to these stresses.

Here we define the role played by MAPK/AP-1 pathways in the response to mitochondrial uncoupling, utilising SH-SY5Y neuroblastoma cells ([35], [36]). Our data suggests a finely balanced system in which feedback loops between c-Jun, Parkin and MAPK activity exist, allowing neurons to rapidly respond to mitochondrial damage and commit to apoptosis if irreversibly damaged. Dysfunction within this multi-faceted process may drive some neurodegenerative pathologies.

2. Materials and methods

2.1. Cell culture

Wild type (WT) and Parkin overexpressing SH-SY5Y neuroblastoma cell lines were obtained from Dr Phil Robinson ([37]), the latter created by stable transfection of a pcDNA3.1/Hygro(+) vector (Invitrogen, Paisley, UK) containing *PARKIN* cDNA into cells followed by hygromycin B selection (Invitrogen). Cells were used between passage 7-16 and grown in DMEM/F12 GlutaMAX™ media supplemented with 10% FCS, 100µg/ml penicillin, 100µg/ml streptomycin and minimum essential media non-essential amino acids (Gibco, Paisley, UK) at 37°C and 5% CO_2. For differentiation, cells were seeded in standard culture medium for 24 hours, then incubated in medium containing 10µM retinoic acid (RA) for 3 days. RA medium was removed, cells washed with PBS then serum-free medium containing 50ng/ml brain derived neurotrophic factor (BDNF) added for 3 days. HEK293 cell lines ([38]) were cultured in DMEM with 10% FCS, 100µg/ml penicillin and 100µg/ml streptomycin (Gibco).

neurotrophic factor (BDNF) added for 5 days. HEK293 cell lines (33) were cultured in DMEM with 10% FCS, 100µg/ml penicillin and 100µg/ml streptomycin (Gibco).

2.2. Antibodies

Antibodies specific for c-Jun (5B1, ab119944), JunD (EPR6520, ab134067), JunB (EPR6518, ab128878), c-Fos (2G2, ab129361), FosB (83B1138, ab11959), Fra-1 (EP4711, ab124722), Fra-2 (EPR4713(2), ab124830), anti-mitochondria [MTCO2] (ab3298) and Histone H3 (1791, ab1791) were obtained from Abcam (Cambridge, UK). Anti-Parkin (Prk8) (4211), -c-Fos (9F6, 2250) and -phosphorylated c-Jun (Ser63) II (9261) obtained from Cell Signalling Technology (Hertfordshire, UK). Anti-β-actin (A5441) was obtained from Sigma. Horseradish-peroxidase anti-mouse (P0260) and anti-rabbit (P0448) secondary antibodies were supplied by Dako (Stockport, UK). Highly-cross adsorbed (H+L) Alexa Fluor 488 anti-mouse (A11029) and Alexa Fluor 594 anti-rabbit (A11037) secondary antibodies from Molecular Probes, Invitrogen.

2.3. Cell proliferation assay

Cells were trypsinised, resuspended in medium then stained with trypan blue and counted using a Countess™ (Invitrogen). 2×10^5 cells/well were seeded and incubated at 37°C for 72 hours. Cells were split and resuspended, then counts performed using a Countess™.

2.4. CCCP assays

Cells were seeded 24 hours before CCCP (Sigma, UK) was added to medium with gentle mixing. Cells scraped into PBS at specific time points and centrifuged at 200xg for 5 min. Pellets frozen at -80°C for protein extraction. Epoxomicin (Santa Cruz Biotechnology, CA, USA) was added 1 hour prior to CCCP addition and SP600125 (JNK inhibitor; Santa Cruz Biotechnology) or FR180204 (ERK inhibitor; Sigma) added 2 hours prior to CCCP.

2.5. Western blotting

Cell pellets were resuspended in ice-cold radioimmunoprecipitation assay buffer (RIPA) buffer (1% Nonidet-P-40, 0.5% sodium deoxycholate and 0.1% SDS in PBS) containing 1X Halt Protease and Phosphatase Inhibitor Cocktail (Pierce, Northumberland, UK) and 5mM EDTA, then left on ice for 30 min. Samples were then centrifuged at 14800xg for 10 min at 4°C and 5µl of supernatant used for a Bradford Assay (BioRad, Hertfordshire, UK) to determine protein concentrations. Remaining supernatant mixed with equal volume of 2X SDS loading buffer containing 0.2M DTT and frozen at -20°C for western blotting.

Using a Mini-Protean II electrophoresis cell (Bio-Rad), protein extracts were subjected to Sodium Dodecyl Sulphate Polyacrylamide Gel Electrophoresis (SDS-PAGE) at 100V in running buffer (25mM Tris base, 250mM glycine, 0.1% SDS). Protein was transferred to Hybond-C extra nitrocellulose membrane (Amersham, Buckinghamshire, UK) at 100V for 90 min in transfer buffer (25mM Tris base, 192mM glycine, 20% methanol, 0.01% SDS). Membranes were blocked in 5% (w/v) milk in PBS for one hour at room temperature (RT) then incubated with primary antibodies prepared at 1:1000 dilutions (β-actin at 1:2000) in block overnight at 4°C. Membranes were washed 6 times in PBS-T then incubated with a 1:2000 dilution of horseradish peroxidase-conjugated secondary antibody in block for 1 hour at RT. Membranes were washed 6 times in PBS-T then once in PBS. Target antigens detected using enhanced chemiluminescence Super Signal West Pico or Femto reagents (Pierce) on a ChemiDoc MP Imaging System with Image Lab 4.0.1 (Bio-Rad) for densitometry.

2.6. Immunofluorescence and CellROX® assays

Cells grown on methanol-sterilised glass coverslip were treated as required then medium removed and washed in PBS, then incubated at RT for 20 min in 4% paraformaldehyde (PFA), washed 3 times in PBS and permeabilised with PBS-0.1% Triton X-100 for 5 min. If required, CellROX® Reagent was added to medium at a final concentration of 5µM 30 minutes prior to fixation. Cells were washed 3 times in PBS then blocked in 0.1% milk powder in PBS for 30 min. Primary antibodies were prepared at 1:1000 dilutions (MTCO2 at 1:500) in block and centrifuged. Coverslips were incubated with primary antibody solutions for 1 hour at RT then washed 3 times in PBS. Secondary antibodies were prepared at 1:500 dilutions in block (DAPI 1:1000) and centrifuged prior to 1 hour incubation with coverslips, which were washed 3 times in PBS after 1 hour. Coverslips mounted using Mowiol.

in PBS. Secondary antibodies were prepared at 1:500 dilutions in block (DAPI 1:1000) and centrifuged prior to 1 hour incubation with coverslips, which were washed 3 times in PBS after 1 hour. Coverslips mounted using Mowiol. Immunostaining was observed using a Nikon Eclipse Ti upright microscope supported by NIS Elements software.

2.7. High-throughput immunofluorescence

Cells were grown and treated in 96-well ViewPlates (PerkinElmer, Berkshire, UK). Fixation, permeabilisation and staining scaled down from above method before PBS added to each well. Plates were processed using the Operetta high-content/high-throughput (HC/HT) wide-field fluorescence imaging system with Harmony software (PerkinElmer) with 20X or 40X objectives (10 or 17 fields of view per well, respectively). Up to 3 fluorescent channels were imaged. Focal planes determined at the start of each experiment. Images were analysed using Columbus software (PerkinElmer) in a non-biased manner. Objects around border of fields of view were excluded. The DAPI channel was used to detect nuclei (>30μm^2 with contrast of over 0.10). Cell counts performed by Columbus software counting nuclei. TOTO3 imaged using far-red illumination. Mitochondria detected using Alexa Fluor 488.

2.8. siRNA knockdown

siRNA SMARTpools obtained from Dharmacon specific to JUN (c-JUN) (M-003268-03-0005), JUNB (M-003269-01-00), JUND (M-003900-05-0005), FOS (c-FOS) (M-003265-01-0005), FOSB (M-010086-03-0005), FOSL1 (FRA-2) (M-004341-04-0005), FOSL2 (FRA-2) (M-004110-00-0005) and PARK2 (PARKIN) (M-003603-00-0005). siRNA specific to non-targeting 1 (NT1) and polo-like kinase 1 (PLK1) were used as negative and positive transfection controls, respectively. A BLAST search was performed (http://blast.ncbi.nlm.nih.gov/Blast.cgi) for individual siRNAs in SMARTpools to predict for off-target effects. Final siRNA concentration was 50nM and carried out in duplicate. RNAiMAX transfection reagent mix was made up in Opti-MEM serum free medium according to manufacturer's instructions. Cells were seeded at 4,000 cells/well using a Fluid-X Xrd-384 dispenser and incubated for 48 hours with siRNA at 37°C in 96 well plates.

2.9. RNA extraction and RT-qPCR

RNA isolation was performed by according to the TRIzol® manufacturers' protocol (Life Technologies), with 1μl of RNase-free glycogen per sample prior to isopropanol and TURBO DNase kit (Ambion, UK) according to the manufacturers' protocol. To quantify RNA, a NanoDrop® ND-1000 Spectrophotometer (Thermo Scientific, Loughborough, UK) was used. A 500ng dilution of RNA was made up in 5μl of RNase-free water, then heated to 65°C for 5 minutes after addition of 1μl random hexamers, 1μl dNTP mix (10mM dA, dC, dG and dT) and 7μl RNase-free water. After 2 minutes on ice, samples were centrifuged then 4μl of 5X 1st strand buffer, 1μl 0.1M DTT and 1μl of SuperScript III reverse transcriptase (200U/μl) were added and incubated for 5 minutes. Samples were heated to 50°C for 50 minutes, followed by 70°C for 15 minutes before cooling on ice.

Reactions were run in duplicate in a MicroAmp® Optical 96-well Reaction Plate (Applied Biosystems, Warrington, UK) with a 20μl final volume in each well (1μl of 20X Taqman® Gene Expression Assay, 10μl of 2X Taqman® Gene Expression Master Mix, 7μl of RNase-free water and 2μl of 1:10 diluted cDNA) using the Taqman recommended qPCR cycle (50°C 2 minutes, 95°C 10 minutes, then; 95°C 15 seconds and annealing/extension at 60°C for 1 minute for 40 cycles) on the ABI 7500 Real Time PCR System (Applied Biosystems) using 7500 SDS software. Primer efficiencies were assessed. To calculate the relative expression level of a gene of interest (GOI) the DDCt method ([39]) was used for primer/probe efficiencies of 100% (-/+10%). To calculate relative expression using primers of <90% efficiency, the standard curve method was employed ([40]) then incorporated as part of the Livak method.

2.10. Statistical Analysis

Independent biological repeats, denoted by 'n' values, refer to complete independent repeats of experiments. Error bars represent standard error of the mean (SEM) or standard deviation (SD) for mean values replicates. Statistical analysis was performed using Prism GraphPad 6 software. Appropriate tests were performed for individual experiments with *post-hoc* analysis if required.

performed using Prism GraphPad 6 software. Appropriate tests were performed for individual experiments with *post-hoc* analysis if required.

3. Results

3.1. Parkin overexpression sensitises cells to mitochondrial uncoupling.

SH-SY5Y cells were used as a neuronal-like model to study the AP-1 response to mitochondrial stress, using CCCP to induce mitochondrial uncoupling and PINK1/Parkin-mediated mitophagy (26-29). Overexpression of Parkin was maintained post-differentiation with RA/BDNF (Fig 1A). Several differentiation protocols were assessed with RA/BDNF inducing the greatest neurite outgrowth (S1 Fig), a characteristic of SNpc dopaminergic neurons (41, 42), so this was chosen for further study. In undifferentiated cells, Parkin overexpression did not alter rate of proliferation (S1 Fig), but did sensitise cells towards differentiation (Fig 1B).

Parkin is generally considered cytoprotective. However, we previously demonstrated that accelerating mitophagy through Parkin overexpression reduced cell viability upon mitochondrial uncoupling in HEK293 cells (38). To investigate the effect of Parkin overexpression in the SH-SY5Y stress response, undifferentiated WT and Parkin overexpressing SH-SY5Y cells were treated with CCCP, H_2O_2 (cellular oxidative stress), rotenone (complex I inhibitor) or epoxomicin (proteasomal inhibition) for 24 hours and surviving cells counted. Parkin specifically sensitised cells to mitochondrial uncoupling, but not other forms of stress (Fig 1C).

CellROX® Green Reagent was used to determine ROS levels over a 24 hour period post-CCCP treatment. Treatment of cells with 5μM CCCP induced oxidative stress, with ROS levels peaking at around 2 hours and resolving back to basal levels by 24 hours (Fig 1D). This was cytotoxic but did not result in the death of the entire cell population after 24h (Fig 1C), thus was chosen for further study.

3.2. c-Jun can act anti- or pro-apoptotically, depending on the mitochondrial stress level.

The Nrf2-mediated antioxidant response is epigenetically repressed in some neurons (43). AP-1-mediation of stress responses may therefore play a more pivotal role in neurons than in other cell types. AP-1 proteins in undifferentiated and differentiated SH-SY5Y cells were observed by immunofluorescence (S2 and S3 Figs). To investigate a functional role for AP-1 transcription factors in the mitochondrial stress response, a targeted siRNA screen was carried out. Individual *JUN* and *FOS* family genes, along with *PARKIN*, were knocked down prior to 24 hour CCCP treatment, then cells fixed, stained for DAPI and counted (Figure 1E). NT-1, a scrambled siRNA control, was used as a siRNA control for comparison. PLK1 knockdown, a positive control for transfection efficacy, resulted in significant cell death. Interestingly, *PARKIN* knockdown did not significantly reduce cell survival after uncoupling compared to control. *c-FOS* siRNA led to significant death in control cells, accounting for lower cell numbers in the CCCP-treated group.

c-Jun is generally considered to be pro-apoptotic under stress conditions in neurons (1, 7, 44-46). In contrast, *c-JUN* knockdown caused an increase in CCCP-induced cell death (Figs 1F and G). However, *c-JUN* knockdown prior to 30mM CCCP conversely reduced cell death (Fig 1H), suggesting a dual role for c-Jun in this context. In cells overexpressing Parkin, knockdown of *c-JUN* did not alter cell survival (Fig 1I).

To further characterise the c-Jun response, western blotting was carried out over a time course. During the first 6 hours in undifferentiated WT cells, no significant change in total c-Jun levels was observed (Fig 2A), but S63 phosphorylated c-Jun became significantly elevated (Fig 2B), the latter even more so in differentiated cells. Parkin overexpression appears to perturb the decline observed in WT cells after their initial increase. Differentiation resulted in an exaggerated c-Jun response, consistent with the hypothesis that it may be more functionally important in neuronal cells. S63 phosphorylated c-Jun/c-Jun ratios also differed between cell lines (Fig 2C).

Over a longer period of uncoupling c-Jun levels were elevated (Fig 3A). Due to the sensitivity of differentiated cells to CCCP, it was only possible to examine this up to 12 hours post-uncoupling. Phosphorylation of c-Jun was distinct in each of 3 cell lines assessed (Fig 3B), as were the phosphorylated c-Jun/c-Jun ratios (Fig 3C). Parkin overexpression again prevented the decline observed in WT cells after their

up to 12 hours post-uncoupling. Phosphorylation of c-Jun was distinct in each of 3 cell lines assessed (Fig 3B), as were the phosphorylated c-Jun/c-Jun ratios (Fig 3C). Parkin overexpression again prevented the decline observed in WT cells after their initial increase Doublets of phosphorylated c-Jun were observed at 2 and 12 hours post-CCCP in differentiated cells, suggesting additional residues were phosphorylated. We also observed modulation of other AP-1 proteins (S4 – S6 Figs).

To monitor changes at transcriptional level, qPCR analysis was employed to assess relative changes in mRNA levels of AP-1 genes. Expression of all 3 *JUN* genes underwent modulation in response to mitochondrial uncoupling (Figs 3D & S7). *c-JUN* expression was regulated in a biphasic manner, with the initial increase in expression detected at 1 hour post-CCCP followed by a drop in mRNA levels between 2 and 6 hours, which was then proceeded by a progressive increase. Changes in *PARKIN* expression showed that the mitophagic response was regulated at the transcriptional level (Fig 3E). To assess the potential c-Jun-mediated apoptotic response relative mRNA levels of *BIM* were assessed, as *BIM* upregulation in response to oxidative stress in neurons by JNK/c-Jun ([47](#)) is critical for neuronal apoptosis ([48](#)). Mitochondrial uncoupling led to a rapid increase in *BIM* expression (Fig 3F), which remained elevated throughout. These data suggested a role for c-Jun in the neuronal response to mitochondrial stress and so we aimed to investigate this further.

3.3. The c-Jun response is differentially regulated by JNK and ERK

AP-1 transcription factors undergo substantial regulation via MAPK-mediated phosphorylation ([11](#)), with JNK considered the primary c-Jun regulator ([49](#)) We therefore investigated the MAPK-dependent modulation of c-Jun by treating cells with SP600125, a JNK inhibitor, or FR180204, an ERK inhibitor, prior to mitochondrial uncoupling. It has been recently shown in SH-SY5Y cells that uncoupling and mitochondrial ATP output is relative to CCCP concentration ([50](#)). We therefore decided to investigate how this would affect MAPK regulation of c-Jun.

Under lower mitochondrial uncoupling (5mM CCCP), JNK and ERK both acted to regulate overall c-Jun levels (Fig 4A). Although JNK inhibition prevented phosphorylation of c-Jun S63, ERK inhibition resulted in greater phosphorylation (Fig 4B), suggesting ERK repressed JNK-mediated phosphorylation of c-Jun. Under higher levels of uncoupling (30mM CCCP), the increase in c-Jun levels was regulated by ERK and supressed by JNK (Fig 4C). The transient boost in c-Jun S63 phosphorylation 2 hours after uncoupling was also mediated by ERK, which again may be antagonised by JNK (Fig 4D). JNK and ERK are therefore likely to both be important under these conditions.

3.4. JNK regulates cell death under high levels of mitochondrial stress in differentiated SH-SY5Y cells.

MAPK inhibition was then examined in differentiated SH-SY5Y cells. JNK inhibition did not have a significant effect on cell death induced by lower uncoupling conditions, but did have a significant effect under higher levels of uncoupling (Figs 5A and 5B), increasing survival by around 6-fold. The lower concentration of JNK inhibitor failed to increase cell survival, as did ERK inhibition. This is consistent with a model in which JNK-regulated apoptosis is only initiated once a critical threshold of mitochondrial damage is passed. Undifferentiated Parkin overexpressing cells were significantly more sensitive to CCCP than WT cells (Fig 1C). This also appeared to be the case in differentiated cells, even with JNK inhibition (Fig 5C).

Complete Parkin-dependent mitophagy requires ubiquitin-proteasome system (UPS) activity, with proteasomal inhibition blocking Parkin activity ([38](#), [51](#)). Autophagic inhibition alone does not perturb UPS-dependent degradation of outer membrane mitochondrial proteins ([52](#)). To investigate if proteasomal dysfunction exacerbated cell death in response to mitochondrial stress and whether this was regulated by MAPK signalling, proteasomal inhibition was induced using epoxomicin. This induced cell death in differentiated WT and Parkin SH-SY5Y cells, which was not rescued by MAPK inhibition (Figs 5D and 5E). However, JNK inhibition did rescue UPS-deficient cells also undergoing mitochondrial uncoupling.

Data from non-neuronal models has demonstrated that mitochondria undergo perinuclear clustering early in mitophagy ([28](#), [53-55](#)). However, in neurons most mitochondria reside within axons and may not undergo somal degradation, with axonal lysosomes and autophagosomes observed ([56-58](#)). Inducing damage in

perinuclear clustering early in mitophagy ([28], [53-55]). However, in neurons most mitochondria reside within axons and may not undergo somal degradation, with axonal lysosomes and autophagosomes observed ([56-58]). Inducing damage in axonal mitochondria leads to rapid local recruitment of Parkin and other mitophagic machinery and localised clustering within autophagosomes ([59]).

We asked whether the inhibition of specific pathways impacted on mitochondrial clustering upon uncoupling. Differentiated WT SH-SY5Y cells underwent uncoupling following MAPK/proteasomal inhibition and mitochondrial clustering was analysed 3 hours after CCCP treatment (Figs 5F, 5G and S8) with TOTO-3 staining labelling the cytoplasm for high-throughput image analysis ([60]). Uncoupling induced a significant increase in the number of mitochondrial clusters (Fig 5G). UPS inhibition reduced mitochondrial clusters post-uncoupling. JNK inhibition reduced mitochondrial clustering in UPS-deficient cells only at the highest level of uncoupling, suggesting that this pathway may only be activated in response to higher levels of mitochondrial damage. Although proteasomal inhibition antagonised mitochondrial clustering, no significant effect was found from the inhibition of either JNK or ERK alone. Thus, MAPK activity does not appear to regulate mitochondrial clustering.

3.5. c-Jun activity under mitochondrial stress may be regulated by Parkin-mediated mitophagy to form a regulatory feedback loop

Parkin overexpressing cells showed a greater increase in c-Jun protein levels 24 hours after mitochondrial uncoupling than WT cells (Fig 3A). c-Jun has previously been shown to repress *PARKIN* expression ([7]). We therefore investigated the link between c-Jun and Parkin-dependent mitophagy. As UPS activation is critical for mitophagy, we tested the effect that proteasomal inhibition had on the c-Jun response to mitochondrial uncoupling. c-Jun protein levels in UPS-deficient cells (Fig 6A) did not show the marginal reduction observed in the normal CCCP response (Fig 2A). Proteasomal inhibition in the absence of uncoupling did not significantly alter c-Jun protein levels (Fig 6B), thus control levels (-/+ epoxomicin) were a comparable basal point. Over a longer period of uncoupling, c-Jun levels became increasingly elevated in UPS-deficient cells (Fig 6C).

To investigate whether a specific functional link between c-Jun and Parkin existed, we used previously characterised HEK293 cell lines that inducibly over-express different Parkin mutants ([38]). Some of these lines expressed non-functional PD-associated *PARKIN* mutations (T240R, R275Y, R42C) or reduced E3 ligase mutants (R42P), allowing us to assess whether modulation of c-Jun levels was dependent on Parkin E3 ligase activity. Compared to untransfected cells, the induction of WT Parkin expression and subsequent mitochondrial uncoupling resulted in a significant increase in c-Jun protein levels (Figs 6D and 6E). Cells expressing R42P Parkin, a functional mutant demonstrating reduced mitophagic activity ([53], [61-63]) exhibited a similar c-Jun induction profile to cells expressing WT Parkin. Expressing mutant forms of Parkin generally resulted in a down regulation of the c-Jun response to mitochondrial uncoupling. Strikingly, inducing the expression of the T240R mutant construct increased the c-Jun response to CCCP-induced stress. Notably, although the R275Y, R42C and T240R mutants are all E3 ligase-deficient, only the latter induced an elevation in c-Jun levels relative to WT Parkin upon uncoupling.

4. Discussion

We aimed to investigate how neuronal decisions to initiate either adaptive or apoptotic responses are made in response to mitochondrial stress. In particular, how mitophagic and signalling pathways interlinked to regulate different arms of the stress response. The SH-SY5Y neuron-like cell line was used to demonstrate the involvement of the JNK/c-Jun pathway in dictating response to mitochondrial dysfunction in a neuronal context. CCCP uncoupled mitochondria and induced oxidative stress and has been shown to induce apoptosis in SH-SY5Y cells at a wide range of concentrations ([64-66]). Utilising both undifferentiated and differentiated cells allowed the identification and functional analysis of MAPK and AP-1 pathways in this response. It also highlighted differences between these cell models, illustrating the importance of choosing an appropriate experimental system in such work. Furthermore, our results, along with previously published works, would suggest that MAPK inhibition may not be an effective therapeutic strategy *in vivo* due to it leading to the downregulation protective pathways, as well as the intended apoptotic pathways.

MAPK inhibition may not be an effective therapeutic strategy *in vivo* due to it leading to the downregulation protective pathways, as well as the intended apoptotic pathways.

4.1. The role of c-Jun is dictated by the level of stress

While many AP-1 transcription factors underwent modulation upon mitochondrial coupling, siRNA knockdowns suggested c-Jun can act in an anti- or pro-apoptotic manner and that this was dependent on the level of mitochondrial damage. This c-Jun response was differentially regulated by JNK and ERK and this regulation was, again, dependent on the level of stress. Parkin overexpression or differentiation towards a more neuronal-like phenotype induced significant alterations in the early c-Jun response to mitochondrial uncoupling. Differentiation resulted in an exaggerated c-Jun response, suggesting it may be more critical in neuronal cells.

Several studies have implicated c-Jun as a pro-apoptotic factor in neuronal and non-neuronal cells undergoing different forms of stress (44-46, 67-69). Initially our results suggested that c-Jun was anti-apoptotic upon mitochondrial uncoupling. Further investigation revealed that under higher levels of mitochondrial dysfunction, c-Jun promoted apoptosis. MAPK/c-Jun activity has recently been shown to regulate both cell death and survival under different levels of PD-associated stress (9). These data suggest biphasic modulation of *c-JUN* expression may allow c-Jun signalling to underpin responses to both lower and higher levels of mitochondrial stress and mediate an apoptotic or cytoprotective response, as appropriate. The level of stress would dictate how c-Jun protein levels and activity were altered. Dysregulation of this biphasic reaction at normally non-cytotoxic levels of mitochondrial damage (e.g. due to UPS dysfunction) could lower the threshold of stress at which c-Jun promotes neuronal apoptosis.

4.2. MAPKs play a critical role in the regulation of c-Jun and the cell death response

Our data revealed both JNK and ERK can regulate c-Jun protein levels and phosphorylation in response to differing levels of mitochondrial stress. It is likely that overall regulation reflects crosstalk between MAPK pathways (16), allowing alternative c-Jun activities to be dictated. Here, JNK-dependent cell death was not initiated by proteasomal dysfunction, but if mitochondrial depolarisation occurred in parallel with UPS-deficiency, the JNK pathway became dominant in inducing cell death. The idea of inhibiting MAPKs such as JNK or ERK has been extensively explored in PD models, however, these data would suggest that inhibition upstream of transcription factors such as c-Jun will in fact lead to the inhibition of numerous other pathways, some of which will not be driving PD pathology.

JNK has been previously proposed as a therapeutic target in neurodegenerative studies as it is generally associated with neuronal death (49, 70). Despite JNK inhibition in animal and cell models yielding promising results, a trial in PD patients involving the kinase inhibitor CEP-1347 was not successful (12). As JNK signalling plays a role in synaptic plasticity (71) and neuronal development (43), as well as our data suggesting it plays a role in the initial adaptive response, inhibition of this whole class of kinases could perturb protective activities that are normally functional in PD neurons. Indeed, it is likely that these endogenous protective pathways are in fact slowing down the progression of neurodegeneration, and thus their perturbation may accelerate disease pathology.

4.3. Parkin and MAPK/AP-1 signalling

Parkin activity has been linked to JNK repression (4, 34, 72-74) and can act both pro- and anti-apoptotically, depending on the level of stress (65). Additionally, JNK stabilises PINK1 under stress (75). Parkin overexpression increases sensitivity to mitochondrial uncoupling in HEK293 cells (38) and SH-SY5Y cells. *BIM*, induced by c-Jun to initiate neuronal apoptosis (45), may regulate crosstalk between autophagy and apoptosis (76, 77) by promoting Parkin recruitment to mitochondria normally perturbed by pro-survival Bcl-2 proteins (66). Indeed, BIM accumulates on the MOM under stress to initiate BAX-dependent cytochrome *c* release (78). Therefore, chronic activation of the JNK/c-Jun pathway may lead to increased BIM-mediated recruitment of Parkin to damaged mitochondria, promoting apoptosis once a threshold of damage is surpassed.

Our data suggests Parkin mutations that perturb its mitochondrial translocation lead to exacerbation of c-Jun signaling upon uncoupling. This is

Our data suggests Parkin mutations that perturb its mitochondrial translocation lead to exacerbation of c-Jun signaling upon uncoupling. This is summarised in Table 1 ([26], [27], [38], [53], [54], [61-63], [79-82]). This perturbation may represent a potential mechanism by which c-Jun-dependent neuronal apoptosis occurs in some PD neurons. As JNK translocation to damaged mitochondria ([83]) induces neuronal apoptosis ([84], [85]) and amplifies mitochondrial ROS production ([86]), it may be critical step in setting the threshold at which irreversible mitochondrial damage has occurred. Parkin could therefore function to regulate mitochondrial JNK signaling to manage the threshold of tolerable damage. When damage levels saturate adaptive responses, excessive mitochondrial JNK would shift the equilibrium towards apoptosis. Therefore, specifically targeting the inhibition of mitochondrial JNK, instead of all cellular JNK, may represent a better therapeutic target in order to prevent any unwanted dampening of JNK-mediated cytoprotection. Indeed, this translocation may be isoform specific, or rely on distinct phosphorylation events, to potentially regulate apoptotic c-Jun signalling. ATF4 upregulates *PARKIN* expression ([7], [8]) and is a critical regulator of the mitochondrial stress response ([87]). As c-Jun represses ATF4-mediated *PARKIN* expression ([7]), regulatory feedback loops would be critical in determining the appropriate pathways to activate (Fig 7). Under excessive stress c-Jun would supress *PARKIN*, antagonising cytoprotective Parkin-mediated mitophagy to facilitate apoptosis of irreversibly damaged cells. The fact we only observed increased apoptosis in Parkin overexpressing cells treated with CCCP and not H_2O_2 or rotenone indicates that this apoptotic promotion by Parkin is not due to oxidative stress, agreeing with previous data ([65]). Therefore, cross-talk between JNK/c-Jun and Parkin pathways could be critical in determining when a switch between adaptive/apoptotic responses occurs.

4.4. Conclusions

Previous studies have shown Parkin to regulate MAPK signalling ([4], [34]). Conversely, *PARKIN* expression can be regulated by the JNK/c-Jun pathway ([7]). ERK has also been shown to localise to damaged mitochondria in order to coordinate mitophagy ([17]). Although our data further suggests a critical role for MAPK/AP-1 in regulating mitochondrial damage-induced cell death, it is clear from additional studies that these pathways also regulate protective stress responses. Therefore, simple kinase inhibition could in fact be detrimental in an *in vivo* setting whereby disease progression occurs over decades due to these protective pathways constantly activating homeostatic mechanisms.

Nigral dopaminergic neurons demonstrate characteristics such higher basal levels of oxidative stress and greater axonal mitochondrial density due to increased bioenergetic demands compared to other neurons ([41]). This combination of factors potentially explains their specific degeneration in PD ([42]). How neuronal fate decisions are made in relation to the type or level of stress remains relatively unexplored. Perturbation of adaptive responses (e.g. by *PARKIN* mutations or non-specific MAPK inhibition) would lower this damage threshold by which apoptosis is activated and in cells such as nigral dopaminergic neurons that are both susceptible to damage and non-renewable this could lead to neurodegeneration.

Previous studies have found that AP-1 proteins FosB, ΔFosB and JunD are involved in long-term neuronal stress adaptations ([88-92]). Here, we focus on early adaptive responses within a novel feedback loop whereby Parkin activity modulates the c-Jun levels in response to mitochondrial stress, potentially relying on the mitochondrial recruitment of Parkin. As ROS is critical in regulating neuronal function ([43], [71]), it is important that stress response feedback loops in neurons function correctly to properly differentiate between survivable and cytotoxic levels of stress. Future work will therefore be crucial to dissect different neuronal pathways and identify specific proteins or events, such as the mitochondrial localisation of specific JNK isoforms and their regulation of c-Jun, that are unique to the neurodegenerative apoptotic responses.

Declarations of interest: None

Declarations of interest: None

References

1.   Hunot S, Vila M, Teismann P, Davis RJ, Hirsch EC, Przedborski S, et al. JNK-mediated induction of cyclooxygenase 2 is required for neurodegeneration in a mouse model of Parkinson's disease. Proceedings of the National Academy of Sciences of the United States of America. 2004;101(2):665-70.

2.   Peng J, Mao XO, Stevenson FF, Hsu M, Andersen JK. The herbicide paraquat induces dopaminergic nigral apoptosis through sustained activation of the JNK pathway. The Journal of biological chemistry. 2004;279(31):32626-32.

3.   Besirli CG, Wagner EF, Johnson EM, Jr. The limited role of NH2-terminal c-Jun phosphorylation in neuronal apoptosis: identification of the nuclear pore complex as a potential target of the JNK pathway. The Journal of cell biology. 2005;170(3):401-11.

4.   Liu M, Aneja R, Sun X, Xie S, Wang H, Wu X, et al. Parkin regulates Eg5 expression by Hsp70 ubiquitination-dependent inactivation of c-Jun NH2-terminal kinase. The Journal of biological chemistry. 2008;283(51):35783-8.

5.   Pan J, Xiao Q, Sheng CY, Hong Z, Yang HQ, Wang G, et al. Blockade of the translocation and activation of c-Jun N-terminal kinase 3 (JNK3) attenuates dopaminergic neuronal damage in mouse model of Parkinson's disease. Neurochemistry international. 2009;54(7):418-25.

6.   Choi WS, Abel G, Klintworth H, Flavell RA, Xia Z. JNK3 mediates paraquat- and rotenone-induced dopaminergic neuron death. Journal of neuropathology and experimental neurology. 2010;69(5):511-20.

7.   Bouman L, Schlierf A, Lutz AK, Shan J, Deinlein A, Kast J, et al. Parkin is transcriptionally regulated by ATF4: evidence for an interconnection between mitochondrial stress and ER stress. Cell death and differentiation. 2011;18(5):769-82.

8.   Sun X, Liu J, Crary JF, Malagelada C, Sulzer D, Greene LA, et al. ATF4 protects against neuronal death in cellular Parkinson's disease models by maintaining levels of parkin. The Journal of neuroscience : the official journal of the Society for Neuroscience. 2013;33(6):2398-407.

9.   Park KH, Shin KS, Zhao TT, Park HJ, Lee KE, Lee MK. L-DOPA modulates cell viability through the ERK-c-Jun system in PC12 and dopaminergic neuronal cells. Neuropharmacology. 2016;101:87-97.

10.   Lee W, Mitchell P, Tjian R. Purified transcription factor AP-1 interacts with TPA-inducible enhancer elements. Cell. 1987;49(6):741-52.

11.   Hess J, Angel P, Schorpp-Kistner M. AP-1 subunits: quarrel and harmony among siblings. Journal of cell science. 2004;117(Pt 25):5965-73.

12.   Parkinson Study Group PI. Mixed lineage kinase inhibitor CEP-1347 fails to delay disability in early Parkinson disease. Neurology. 2007;69(15):1480-90.

13.   Cargnello M, Roux PP. Activation and function of the MAPKs and their substrates, the MAPK-activated protein kinases. Microbiol Mol Biol Rev. 2011;75(1):50-83.

14.   Peng J, Andersen JK. The role of c-Jun N-terminal kinase (JNK) in Parkinson's disease. IUBMB life. 2003;55(4-5):267-71.

15.   Lopez-Bergami P, Huang C, Goydos JS, Yip D, Bar-Eli M, Herlyn M, et al. Rewired ERK-JNK signaling pathways in melanoma. Cancer Cell. 2007;11(5):447-60.

16.   Fey D, Croucher DR, Kolch W, Kholodenko BN. Crosstalk and signaling switches in mitogen-activated protein kinase cascades. Front Physiol. 2012;3:355.

17.   Dagda RK, Zhu J, Kulich SM, Chu CT. Mitochondrially localized ERK2 regulates mitophagy and autophagic cell stress: implications for Parkinson's disease. Autophagy. 2008;4(6):770-82.

18.   Pyakurel A, Savoia C, Hess D, Scorrano L. Extracellular regulated kinase phosphorylates mitofusin 1 to control mitochondrial morphology and apoptosis. Mol Cell. 2015;58(2):244-54.

19.   Kultz D. Molecular and evolutionary basis of the cellular stress response. Annu Rev Physiol. 2005;67:225-57.

20.   Fulda S, Gorman AM, Hori O, Samali A. Cellular stress responses: cell survival and cell death. Int J Cell Biol. 2010;2010:214074.

21.   Finkel T, Holbrook NJ. Oxidants, oxidative stress and the biology of ageing. Nature. 2000;408(6809):239-47.

22.   Lemasters JJ. Selective mitochondrial autophagy, or mitophagy, as a targeted defense against oxidative stress, mitochondrial dysfunction, and aging. Rejuvenation research. 2005;8(1):3-5.

22.   Lemasters JJ. Selective mitochondrial autophagy, or mitophagy, as a targeted defense against oxidative stress, mitochondrial dysfunction, and aging. Rejuvenation research. 2005;8(1):3-5.

23.   Deas E, Wood NW, Plun-Favreau H. Mitophagy and Parkinson's disease: the PINK1-parkin link. Biochimica et biophysica acta. 2011;1813(4):623-33.

24.   Kitada T, Asakawa S, Hattori N, Matsumine H, Yamamura Y, Minoshima S, et al. Mutations in the parkin gene cause autosomal recessive juvenile parkinsonism. Nature. 1998;392(6676):605-8.

25.   Scarffe LA, Stevens DA, Dawson VL, Dawson TM. Parkin and PINK1: much more than mitophagy. Trends Neurosci. 2014;37(6):315-24.

26.   Matsuda N, Sato S, Shiba K, Okatsu K, Saisho K, Gautier CA, et al. PINK1 stabilized by mitochondrial depolarization recruits Parkin to damaged mitochondria and activates latent Parkin for mitophagy. The Journal of cell biology. 2010;189(2):211-21.

27.   Narendra DP, Jin SM, Tanaka A, Suen DF, Gautier CA, Shen J, et al. PINK1 is selectively stabilized on impaired mitochondria to activate Parkin. PLoS biology. 2010;8(1):e1000298.

28.   Vives-Bauza C, Zhou C, Huang Y, Cui M, de Vries RL, Kim J, et al. PINK1-dependent recruitment of Parkin to mitochondria in mitophagy. Proceedings of the National Academy of Sciences of the United States of America. 2010;107(1):378-83.

29.   Narendra D, Tanaka A, Suen DF, Youle RJ. Parkin is recruited selectively to impaired mitochondria and promotes their autophagy. The Journal of cell biology. 2008;183(5):795-803.

30.   Ichijo H, Nishida E, Irie K, ten Dijke P, Saitoh M, Moriguchi T, et al. Induction of apoptosis by ASK1, a mammalian MAPKKK that activates SAPK/JNK and p38 signaling pathways. Science. 1997;275(5296):90-4.

31.   Tobiume K, Matsuzawa A, Takahashi T, Nishitoh H, Morita K, Takeda K, et al. ASK1 is required for sustained activations of JNK/p38 MAP kinases and apoptosis. EMBO reports. 2001;2(3):222-8.

32.   Zhang Q, Zhang G, Meng F, Tian H. Biphasic activation of apoptosis signal-regulating kinase 1-stress-activated protein kinase 1-c-Jun N-terminal protein kinase pathway is selectively mediated by Ca2+-permeable alpha-amino-3-hydroxy-5-methyl-4-isoxazolepropionate receptors involving oxidative stress following brain ischemia in rat hippocampus. Neurosci Lett. 2003;337(1):51-5.

33.   Hu X, Weng Z, Chu CT, Zhang L, Cao G, Gao Y, et al. Peroxiredoxin-2 protects against 6-hydroxydopamine-induced dopaminergic neurodegeneration via attenuation of the apoptosis signal-regulating kinase (ASK1) signaling cascade. J Neurosci. 2011;31(1):247-61.

34.   Cha GH, Kim S, Park J, Lee E, Kim M, Lee SB, et al. Parkin negatively regulates JNK pathway in the dopaminergic neurons of Drosophila. Proceedings of the National Academy of Sciences of the United States of America. 2005;102(29):10345-50.

35.   Biedler JL, Helson L, Spengler BA. Morphology and growth, tumorigenicity, and cytogenetics of human neuroblastoma cells in continuous culture. Cancer research. 1973;33(11):2643-52.

36.   Xie HR, Hu LS, Li GY. SH-SY5Y human neuroblastoma cell line: in vitro cell model of dopaminergic neurons in Parkinson's disease. Chinese medical journal. 2010;123(8):1086-92.

37.   Pennington K, Peng J, Hung CC, Banks RE, Robinson PA. Differential effects of wild-type and A53T mutant isoform of alpha-synuclein on the mitochondrial proteome of differentiated SH-SY5Y cells. Journal of proteome research. 2010;9(5):2390-401.

38.   Morrison E, Thompson J, Williamson SJ, Cheetham ME, Robinson PA. A simple cell based assay to measure Parkin activity. Journal of neurochemistry. 2011;116(3):342-9.

39.   Livak KJ, Schmittgen TD. Analysis of relative gene expression data using real-time quantitative PCR and the 2(-Delta Delta C(T)) Method. Methods. 2001;25(4):402-8.

40.   Pfaffl MW. A new mathematical model for relative quantification in real-time RT-PCR. Nucleic Acids Res. 2001;29(9):e45.

41.   Matsuda W, Furuta T, Nakamura KC, Hioki H, Fujiyama F, Arai R, et al. Single nigrostriatal dopaminergic neurons form widely spread and highly dense axonal arborizations in the neostriatum. J Neurosci. 2009;29(2):444-53.

42.   Pacelli C, Giguere N, Bourque MJ, Levesque M, Slack RS, Trudeau LE. Elevated Mitochondrial Bioenergetics and Axonal Arborization Size Are Key Contributors to the Vulnerability of Dopamine Neurons. Curr Biol. 2015.

42.	Pacelli C, Giguere N, Bourque MJ, Levesque M, Slack RS, Trudeau LE. Elevated Mitochondrial Bioenergetics and Axonal Arborization Size Are Key Contributors to the Vulnerability of Dopamine Neurons. Curr Biol. 2015.

43.	Bell KF, Al-Mubarak B, Martel MA, McKay S, Wheelan N, Hasel P, et al. Neuronal development is promoted by weakened intrinsic antioxidant defences due to epigenetic repression of Nrf2. Nat Commun. 2015;6:7066.

44.	Ham J, Babij C, Whitfield J, Pfarr CM, Lallemand D, Yaniv M, et al. A c-Jun dominant negative mutant protects sympathetic neurons against programmed cell death. Neuron. 1995;14(5):927-39.

45.	Whitfield J, Neame SJ, Paquet L, Bernard O, Ham J. Dominant-negative c-Jun promotes neuronal survival by reducing BIM expression and inhibiting mitochondrial cytochrome c release. Neuron. 2001;29(3):629-43.

46.	Wilhelm M, Xu Z, Kukekov NV, Gire S, Greene LA. Proapoptotic Nix activates the JNK pathway by interacting with POSH and mediates death in a Parkinson disease model. J Biol Chem. 2007;282(2):1288-95.

47.	Jin HO, Park IC, An S, Lee HC, Woo SH, Hong YJ, et al. Up-regulation of Bak and Bim via JNK downstream pathway in the response to nitric oxide in human glioblastoma cells. J Cell Physiol. 2006;206(2):477-86.

48.	Putcha GV, Moulder KL, Golden JP, Bouillet P, Adams JA, Strasser A, et al. Induction of BIM, a proapoptotic BH3-only BCL-2 family member, is critical for neuronal apoptosis. Neuron. 2001;29(3):615-28.

49.	Borsello T, Forloni G. JNK signalling: a possible target to prevent neurodegeneration. Curr Pharm Des. 2007;13(18):1875-86.

50.	Park YS, Choi SE, Koh HC. PGAM5 regulates PINK1/Parkin-mediated mitophagy via DRP1 in CCCP-induced mitochondrial dysfunction. Toxicol Lett. 2018;284:120-8.

51.	Chan NC, Salazar AM, Pham AH, Sweredoski MJ, Kolawa NJ, Graham RL, et al. Broad activation of the ubiquitin-proteasome system by Parkin is critical for mitophagy. Human molecular genetics. 2011;20(9):1726-37.

52.	Yoshii SR, Kishi C, Ishihara N, Mizushima N. Parkin mediates proteasome-dependent protein degradation and rupture of the outer mitochondrial membrane. J Biol Chem. 2011;286(22):19630-40.

53.	Narendra D, Kane LA, Hauser DN, Fearnley IM, Youle RJ. p62/SQSTM1 is required for Parkin-induced mitochondrial clustering but not mitophagy; VDAC1 is dispensable for both. Autophagy. 2010;6(8):1090-106.

54.	Okatsu K, Saisho K, Shimanuki M, Nakada K, Shitara H, Sou YS, et al. p62/SQSTM1 cooperates with Parkin for perinuclear clustering of depolarized mitochondria. Genes Cells. 2010;15(8):887-900.

55.	Shi J, Fung G, Deng H, Zhang J, Fiesel FC, Springer W, et al. NBR1 is dispensable for PARK2-mediated mitophagy regardless of the presence or absence of SQSTM1. Cell Death Dis. 2015;6:e1943.

56.	Lee S, Sato Y, Nixon RA. Lysosomal proteolysis inhibition selectively disrupts axonal transport of degradative organelles and causes an Alzheimer's-like axonal dystrophy. J Neurosci. 2011;31(21):7817-30.

57.	Lee S, Sato Y, Nixon RA. Primary lysosomal dysfunction causes cargo-specific deficits of axonal transport leading to Alzheimer-like neuritic dystrophy. Autophagy. 2011;7(12):1562-3.

58.	Maday S, Wallace KE, Holzbaur EL. Autophagosomes initiate distally and mature during transport toward the cell soma in primary neurons. J Cell Biol. 2012;196(4):407-17.

59.	Ashrafi G, Schlehe JS, LaVoie MJ, Schwarz TL. Mitophagy of damaged mitochondria occurs locally in distal neuronal axons and requires PINK1 and Parkin. The Journal of cell biology. 2014;206(5):655-70.

60.	Wheway G, Schmidts M, Mans DA, Szymanska K, Nguyen TT, Racher H, et al. An siRNA-based functional genomics screen for the identification of regulators of ciliogenesis and ciliopathy genes. Nat Cell Biol. 2015;17(8):1074-87.

61.	Terreni L, Calabrese E, Calella AM, Forloni G, Mariani C. New mutation (R42P) of the parkin gene in the ubiquitinlike domain associated with parkinsonism. Neurology. 2001;56(4):463-6.

62.	Geisler S, Holmstrom KM, Skujat D, Fiesel FC, Rothfuss OC, Kahle PJ, et al. PINK1/Parkin-mediated mitophagy is dependent on VDAC1 and p62/SQSTM1. Nature cell biology. 2010;12(2):119-31.

63.	Lee JY, Nagano Y, Taylor JP, Lim KL, Yao TP. Disease-causing mutations in parkin impair mitochondrial ubiquitination, aggregation, and HDAC6-dependent mitophagy. J Cell Biol. 2010;189(4):671-9.

64.	Arena G, Gelmetti V, Torosantucci L, Vignone D, Lamorte G, De Rosa P, et

in parkin-impair mitochondrial ubiquitination, aggregation, and HDAC6-dependent mitophagy. J Cell Biol. 2010;189(4):671-9.

64.	Arena G, Gelmetti V, Torosantucci L, Vignone D, Lamorte G, De Rosa P, et al. PINK1 protects against cell death induced by mitochondrial depolarization, by phosphorylating Bcl-xL and impairing its pro-apoptotic cleavage. Cell Death Differ. 2013;20(7):920-30.

65.	Carroll RG, Hollville E, Martin SJ. Parkin sensitizes toward apoptosis induced by mitochondrial depolarization through promoting degradation of Mcl-1. Cell Rep. 2014;9(4):1538-53.

66.	Hollville E, Carroll RG, Cullen SP, Martin SJ. Bcl-2 family proteins participate in mitochondrial quality control by regulating Parkin/PINK1-dependent mitophagy. Molecular cell. 2014;55(3):451-66.

67.	Watson A, Eilers A, Lallemand D, Kyriakis J, Rubin LL, Ham J. Phosphorylation of c-Jun is necessary for apoptosis induced by survival signal withdrawal in cerebellar granule neurons. The Journal of neuroscience : the official journal of the Society for Neuroscience. 1998;18(2):751-62.

68.	Ham J, Eilers A, Whitfield J, Neame SJ, Shah B. c-Jun and the transcriptional control of neuronal apoptosis. Biochem Pharmacol. 2000;60(8):1015-21.

69.	Gearan T, Castillo OA, Schwarzschild MA. The parkinsonian neurotoxin, MPP+ induces phosphorylated c-Jun in dopamingric neurons of mesencephalic cultures. Parkinsonism Relat Disord. 2001;8(1):19-22.

70.	Spigolon G, Cavaccini A, Trusel M, Tonini R, Fisone G. cJun N-terminal kinase (JNK) mediates cortico-striatal signaling in a model of Parkinson's disease. Neurobiol Dis. 2018;110:37-46.

71.	Milton VJ, Jarrett HE, Gowers K, Chalak S, Briggs L, Robinson IM, et al. Oxidative stress induces overgrowth of the Drosophila neuromuscular junction. Proceedings of the National Academy of Sciences of the United States of America. 2011;108(42):17521-6.

72.	Jiang H, Ren Y, Zhao J, Feng J. Parkin protects human dopaminergic neuroblastoma cells against dopamine-induced apoptosis. Human molecular genetics. 2004;13(16):1745-54.

73.	Ren Y, Jiang H, Yang F, Nakaso K, Feng J. Parkin protects dopaminergic neurons against microtubule-depolymerizing toxins by attenuating microtubule-associated protein kinase activation. J Biol Chem. 2009;284(6):4009-17.

74.	Hwang S, Kim D, Choi G, An SW, Hong YK, Suh YS, et al. Parkin suppresses c-Jun N-terminal kinase-induced cell death via transcriptional regulation in Drosophila. Mol Cells. 2010;29(6):575-80.

75.	Park JH, Ko J, Park YS, Park J, Hwang J, Koh HC. Clearance of Damaged Mitochondria Through PINK1 Stabilization by JNK and ERK MAPK Signaling in Chlorpyrifos-Treated Neuroblastoma Cells. Mol Neurobiol. 2017;54(3):1844-57.

76.	Luo S, Garcia-Arencibia M, Zhao R, Puri C, Toh PP, Sadiq O, et al. Bim inhibits autophagy by recruiting Beclin 1 to microtubules. Mol Cell. 2012;47(3):359-70.

77.	Luo S, Rubinsztein DC. BCL2L11/BIM: a novel molecular link between autophagy and apoptosis. Autophagy. 2013;9(1):104-5.

78.	Renault TT, Floros KV, Elkholi R, Corrigan KA, Kushnareva Y, Wieder SY, et al. Mitochondrial shape governs BAX-induced membrane permeabilization and apoptosis. Mol Cell. 2015;57(1):69-82.

79.	Avraham E, Rott R, Liani E, Szargel R, Engelender S. Phosphorylation of Parkin by the cyclin-dependent kinase 5 at the linker region modulates its ubiquitin-ligase activity and aggregation. J Biol Chem. 2007;282(17):12842-50.

80.	Ko HS, Lee Y, Shin JH, Karuppagounder SS, Gadad BS, Koleske AJ, et al. Phosphorylation by the c-Abl protein tyrosine kinase inhibits parkin's ubiquitination and protective function. Proceedings of the National Academy of Sciences of the United States of America. 2010;107(38):16691-6.

81.	Rose JM, Novoselov SS, Robinson PA, Cheetham ME. Molecular chaperone-mediated rescue of mitophagy by a Parkin RING1 domain mutant. Hum Mol Genet. 2011;20(1):16-27.

82.	Veeriah S, Taylor BS, Meng S, Fang F, Yilmaz E, Vivanco I, et al. Somatic mutations of the Parkinson's disease-associated gene PARK2 in glioblastoma and other human malignancies. Nat Genet. 2010;42(1):77-82.

83.	Wiltshire C, Gillespie DA, May GH. Sab (SH3BP5), a novel mitochondria-localized JNK-interacting protein. Biochem Soc Trans. 2004;32(Pt 6):1075-7.

84.	Chambers JW, Pachori A, Howard S, Ganno M, Hansen D, Jr., Kamenecka T, et al. Small Molecule c-jun-N-terminal Kinase (JNK) Inhibitors Protect

localized JNK-interacting protein. Biochem Soc Trans. 2004;32(Pt 6):1075-7.

84. Chambers JW, Pachori A, Howard S, Ganno M, Hansen D, Jr., Kamenecka T, et al. Small Molecule c-jun-N-terminal Kinase (JNK) Inhibitors Protect Dopaminergic Neurons in a Model of Parkinson's Disease. ACS Chem Neurosci. 2011;2(4):198-206.

85. Chambers JW, Howard S, LoGrasso PV. Blocking c-Jun N-terminal kinase (JNK) translocation to the mitochondria prevents 6-hydroxydopamine-induced toxicity in vitro and in vivo. J Biol Chem. 2013;288(2):1079-87.

86. Chambers JW, LoGrasso PV. Mitochondrial c-Jun N-terminal kinase (JNK) signaling initiates physiological changes resulting in amplification of reactive oxygen species generation. J Biol Chem. 2011;286(18):16052-62.

87. Quiros PM, Prado MA, Zamboni N, D'Amico D, Williams RW, Finley D, et al. Multi-omics analysis identifies ATF4 as a key regulator of the mitochondrial stress response in mammals. J Cell Biol. 2017;216(7):2027-45.

88. Chen J, Nye HE, Kelz MB, Hiroi N, Nakabeppu Y, Hope BT, et al. Regulation of delta FosB and FosB-like proteins by electroconvulsive seizure and cocaine treatments. Mol Pharmacol. 1995;48(5):880-9.

89. Hiroi N, Marek GJ, Brown JR, Ye H, Saudou F, Vaidya VA, et al. Essential role of the fosB gene in molecular, cellular, and behavioral actions of chronic electroconvulsive seizures. J Neurosci. 1998;18(17):6952-62.

90. Nestler EJ, Barrot M, Self DW. DeltaFosB: a sustained molecular switch for addiction. Proc Natl Acad Sci U S A. 2001;98(20):11042-6.

91. Pavon N, Martin AB, Mendialdua A, Moratalla R. ERK phosphorylation and FosB expression are associated with L-DOPA-induced dyskinesia in hemiparkinsonian mice. Biol Psychiatry. 2006;59(1):64-74.

92. Cao X, Yasuda T, Uthayathas S, Watts RL, Mouradian MM, Mochizuki H, et al. Striatal overexpression of DeltaFosB reproduces chronic levodopa-induced involuntary movements. J Neurosci. 2010;30(21):7335-43.

	Parkin mutant													
	WT	R275Y	T240R	S131A	Y143F	R42P	R42C	R275W	T415N	C289G	G430D	C352G	K161N	K211N
Region of mutation	n/a	RING1	RING1	SH2-like domain	SH2-like domain	UBL domain	UBL domain	RING1	RING2	RING1	RING2	IBR domain	SH2-like domain	SH2-like domain
E3 ubiquitin ligase activity	✓	✗	✗	✓	✓	✓	?	✗	✗	?	✗	✗	✗	✗
Mitophagy blocked by proteasomal inhibition	✓	n/a	n/a	✓	✗	✓	n/a	n/a	n/a	n/a	n/a	n/a	n/a	n/a
Recruited to depolarised mitochondria	✓	?	✗	✓	✓	✓	✓	✓	✓	✗	✗ ✓	✓	✓	✗
Induces mitochondrial clustering	✓	✗	✗	✓	✓	✓	✓	Delayed	✓ ✗	✗	✗	✗	✓	✗

Induces mitochondrial clustering	✓	✗	✗	✓	✓	✓	✓	Delayed	✓ ✗	✗	✗	✗	✗	✓	✗
Induces mitochondrial degradation	✓	✗	✗	✓	✓	✓	✗	✗	✗	✗	✗	✗	✗	✗	✗
Change in c-Jun levels 24h post-CCCP (relative to WT)	n/a	Decrease	Increase	Decrease	Decrease	No change	Decrease	?	?	?	?	?	?	?	

Table 1: Parkin mutations perturb mitophagy at different stages. Previous data demonstrates that dysfunction occurs at different stages of mitophagy depending on the Parkin mutant. To date, the steps at which this disruption occurs for each mutant shown here has not been fully elucidated. Our data suggests that Parkin translocation to mitochondria upon uncoupling may be critical in the regulation of c-Jun. Note: some studies demonstrate contradictory data and some boxes therefore contain both ticks and crosses. n/a = not available. '?' represents unknown.
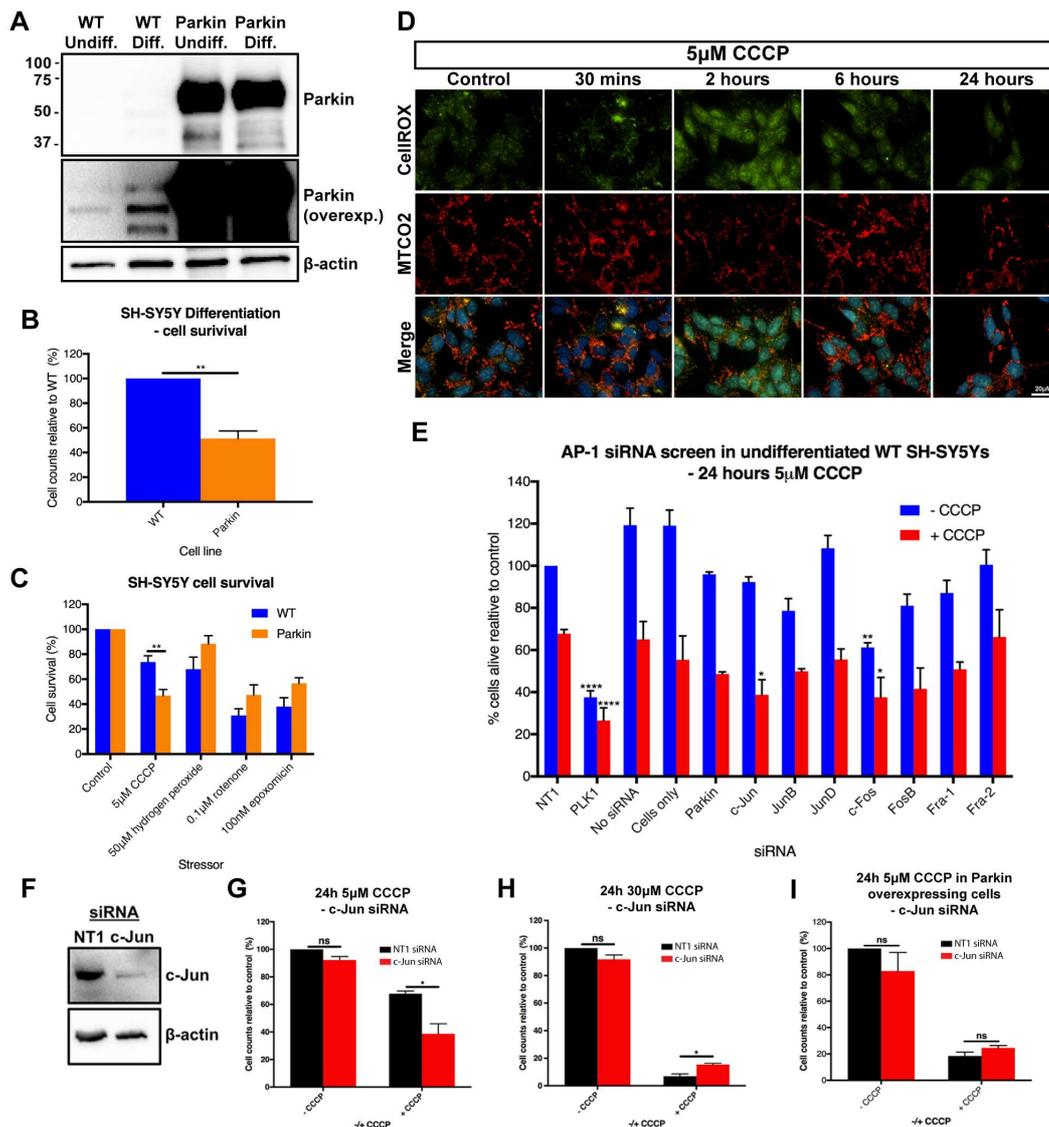
Figure 1: Parkin and c-Jun play a role in CCCP-induced apoptosis. SH-SY5Y cells in undifferentiated form or differentiated form (differentiated by 10µM retinoic acid (RA) for 3 days (10% serum) followed by 50ng/ml BDNF (no serum) for 3 days). (A) Western blot analysis revealed Parkin overexpression was maintained post-differentiation. (B) Parkin overexpression resulted in greater sensitivity to RA/BDNF differentiation. DAPI counts were performed using an Operetta system (n = 3) and analysed using an unpaired two-tailed t-test (****p < 0.001). (C) Parkin overexpression rendered undifferentiated cells more sensitive to mitochondrial uncoupling. Cells plated at 4,000 cells/well for 24 hours were then exposed to 5µM CCCP, 50µM H_2O_2, 0.1µM rotenone or 100nM epoxomicin over a 24-hour period, then fixed and stained with DAPI and counts performed on an Operetta system (n = 4). Statistical significance was ascertained using a 2way ANOVA (Bonferroni's) (*p<0.05, **p<0.01). (D) Treatment of SH-SY5Y cells with 5µM CCCP induced oxidative stress. Cells were stained with the mitochondrial marker MTCO2 (red), CellROX® (green) and DAPI (blue). CellROX® Green staining showed (E) Knockdown by siRNA SMARTpools was performed 48 hours prior to CCCP challenge and cell counts (relative to DMSO-treated NT-1 knockdown cells) performed on an Operetta imaging system using DAPI-stained nuclei (n = 3). A siRNA screen of the AP-1 proteins and Parkin, using NT1 (non-targeting 1) and PLK1 (polo-like kinases) as negative and transfection controls respectively, showed c-Jun may play a role in the cell death response to mitochondrial uncoupling. (F) Knockdown of c-Jun was confirmed by
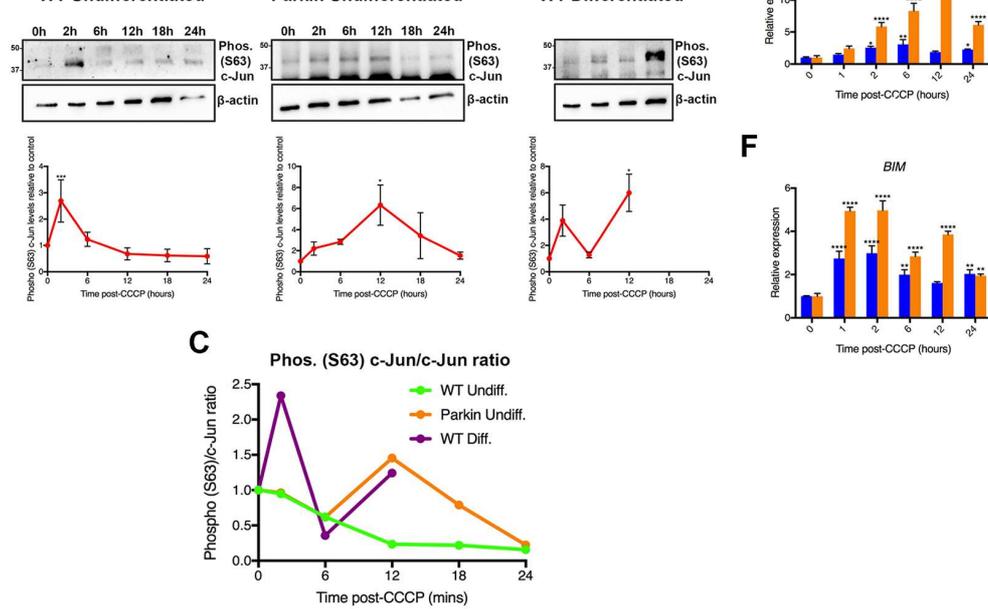
of the AP-1 proteins and Parkin, using NT1 (non-targeting 1) and PLK1 (polo-like kinases) as negative and transfection controls respectively, showed c-Jun may play a role in the cell death response to mitochondrial uncoupling. (F) Knockdown of c-Jun was confirmed by western blot. Cell death for knockdowns was quantified using the Operetta system. (G) siRNA knockdown of c-Jun resulted in increased death induced by 5μM CCCP. (H) Under 30μM CCCP conditions, knockdown of c-Jun reduced cell death. (I) No significant alteration to the level of cell death was observed after c-Jun was knocked down prior to uncoupling in Parkin overexpressing cells. Statistical significance was assessed using an unpaired 2-tailed t-test (*$p<0.05$). Error bars represent SEM.

Figure 2: c-Jun is rapidly modulated in response to mitochondrial uncoupling. Western blot analysis was carried out on protein extracts obtained at specific time points after the treatment of undifferentiated/differentiated WT or undifferentiated Parkin overexpressing SH-SY5Y cells with 5mM CCCP over a 6 hour period. Where required, cells were differentiated in 10μM RA for 3 days (10% serum) followed by 50ng/ml BDNF (no serum) for 3 days prior to treatment with CCCP. Densitometry was calculated relative to the loading control ($n = 3$). (A) Statistically significant changes in c-Jun protein levels were observed in Parkin and differentiated SH-SY5Y lines. (B) Phosphorylated (S63) c-Jun levels show significant elevation after uncoupling. (C) Average values for total c-Jun and phosphorylated (S63) c-Jun levels were used to calculate the phospho/total c-Jun ratio over the first 6 hours of uncoupling. Statistical significance was determined using a 2way ANOVA (Dunnett's) (*$p<0.05$, **$p<0.01$, ***$p<0.005$). Quantified levels were compared to levels at time point 0. Error bars represent SEM.
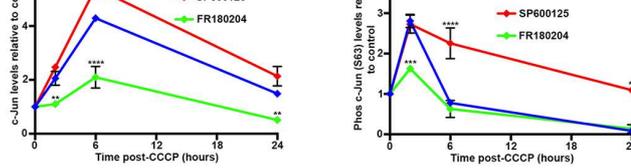
Figure 3: The c-Jun response to mitochondrial uncoupling is variably modulated over the 24 hour period of stress. Western blot analysis was carried out on protein extracts obtained at specific time points after the treatment of undifferentiated/differentiated WT or undifferentiated Parkin overexpressing SH-SY5Y cells with 5mM CCCP over a 24 hour period (*n* = 3). Where required, cells were differentiated in 10µM RA for 3 days (10% serum) followed by 50ng/ml BDNF (no serum) for 3 days prior to treatment with CCCP. Differentiated cells were highly sensitive to CCCP challenge and a sufficient quantity of extract was only obtained up to the 12 hour time point. Densitometry was calculated relative to the loading control. (A) Significant increases in c-Jun levels were observed in all 3 cell lines undergoing uncoupling. (B) Phosphorylated (S63) c-Jun levels showed more significant elevation in differentiated cells.. (C) Average values for total c-Jun and phosphorylated (S63) c-Jun levels were used to calculate the phospho/total c-Jun ratio over 24 hours of uncoupling. (D-E) cDNA obtained from RNA extracts over the 24h after 5mM CCCP challenge in undifferentiated WT SH-SY5Y cells was analysed for relative expression of the individual AP-1 genes by qPCR. Expression levels are relative to the 0h time point. (D) *c-JUN* expression was regulated in a biphasic manner upon uncoupling. (E) *PARKIN* expression was upregulated in response to mitochondrial uncoupling. (F) *BIM* expression was upregulated within 1h of uncoupling, before dropping. qPCR Graphs show 2 independent biological repeats (1st – blue, 2nd – orange) with errors bars representing variation between technical replicates within a single experiment. Statistical significance was determined using a 2way ANOVA (Dunnett's) (*p<0.05, **p<0.01, ***p<0.005, ****p<0.001). Quantified levels were compared to levels at time point 0. Error bars represent SEM (westerns) or SD (qPCR).
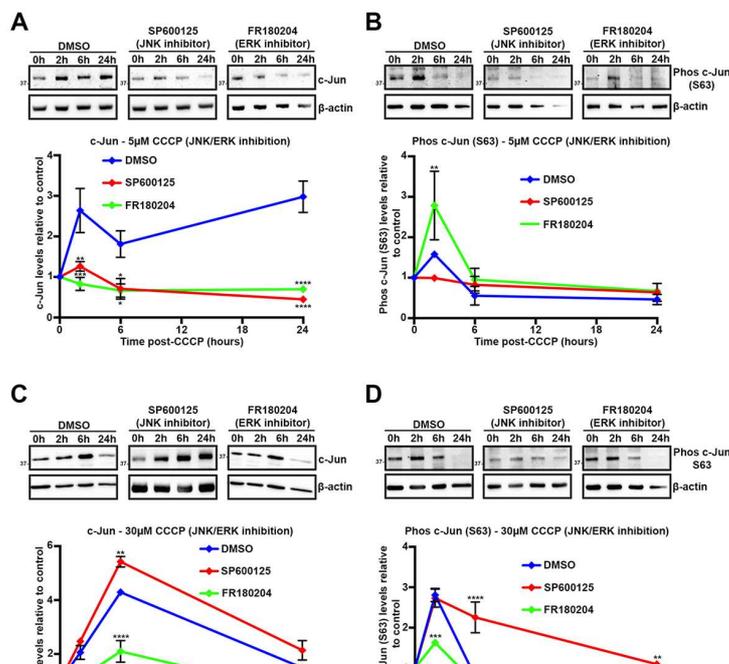
Figure 4: JNK and ERK modulate c-Jun levels in response to different levels of mitochondrial stress. Western blot analysis was carried out on extracts obtained at different time points from undifferentiated WT SH-SY5Y cells that were treated with 10μM SP600125 or 1μM FR180204 2h prior to challenge with CCCP. (A) Inhibition of both JNK and ERK suppressed the increase in c-Jun levels seen in response to 5μM CCCP. (B) Following challenge with 5μM CCCP, JNK inihibition decreased c-Jun S63 phosphorylation, whereas ERK inhibition increased it. (C) In response to 30μM CCCP, ERK-induced c-Jun upregulation was perturbed by JNK activity. (D) ERK activity regulated transient c-Jun S63 phosphorylation in response to higher levels of uncoupling, while JNK contributed to the regulation of this phosphorylation (*n* = 2). Statistical significance was determined using a 2-way ANOVA (Tukey's) relative to the inhibitor vehicle control (DMSO) at each time point (*$p<0.05$, **$p<0.01$, ***$p<0.005$, ****$p<0.001$). Error bars represent SEM.
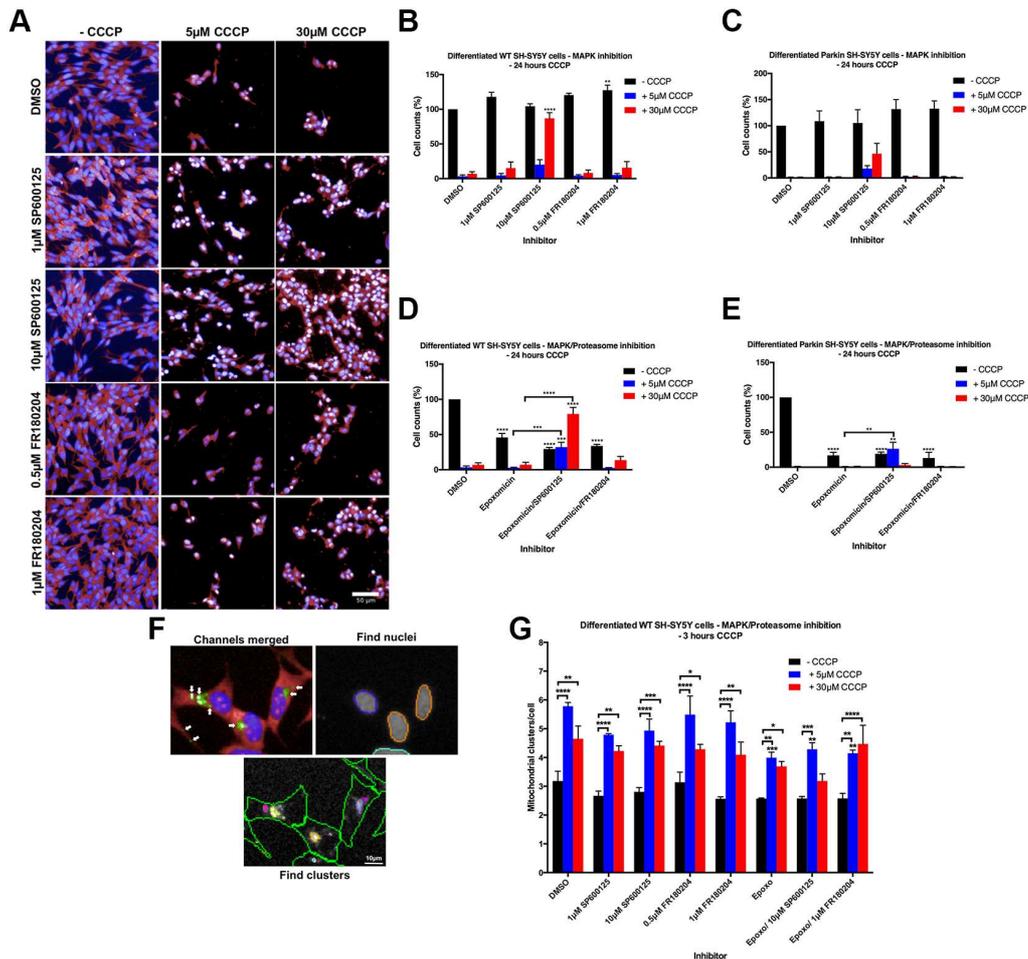
Figure 5: JNK promotes apoptosis in differentiated WT SH-SY5Y cells in response to high levels of mitochondrial stress. Cells were differentiated in 10μM RA for 3 days (10% serum) followed by 50ng/ml BDNF (no serum) for 3 days in 96-well Operetta plates, then treated with SP600125 (JNK inhibitor), FR180204 (ERK inhibitor) and/or 100nM epoxomicin (proteasomal inhibitor) prior to CCCP exposure. Images were captured using an Operetta imaging system and analysed using Columbus software. Nuclei stained with DAPI (blue) and cytoplasm with TOTO-3 (cytoplasm). (A) Examples of images captured on the Operetta at 20X magnification. (B) A significant rescue in cell numbers by JNK inhibition was only seen in cultures challenged with high levels of CCCP (*n* = 4). (C) MAPK inhibition in differentiated Parkin overexpressing SH-SY5Y cells (*n* = 4). (D & E) JNK-mediated apoptosis did not occur in differentiated WT cells undergoing proteasomal inhibition, but was initiated upon the addition of mitochondrial uncoupling (*n* = 4). (F & G) Columbus software was used to analyse images captured using the Operetta. Mitochondrial clusters on the FITC channel (green) within the cytoplasm (TOTO3 – red) were labelled and counted relative to nuclei on the DAPI channel. Mitochondrial clustering 3h post-CCCP challenge in differentiated WT SH-SY5Y cells was perturbed by proteasomal inhibition but not MAPK inhibition (*n* = 3). Statistical significance was determined using a 2-way ANOVA (Tukey's) (*$p<0.05$, **$p<0.01$, ***$p<0.005$, ****$p<0.001$). Comparisons were made between inhibitor-treatment and inhibitor vehicle control of the same CCCP concentration, unless otherwise indicated by horizontal bars. Error
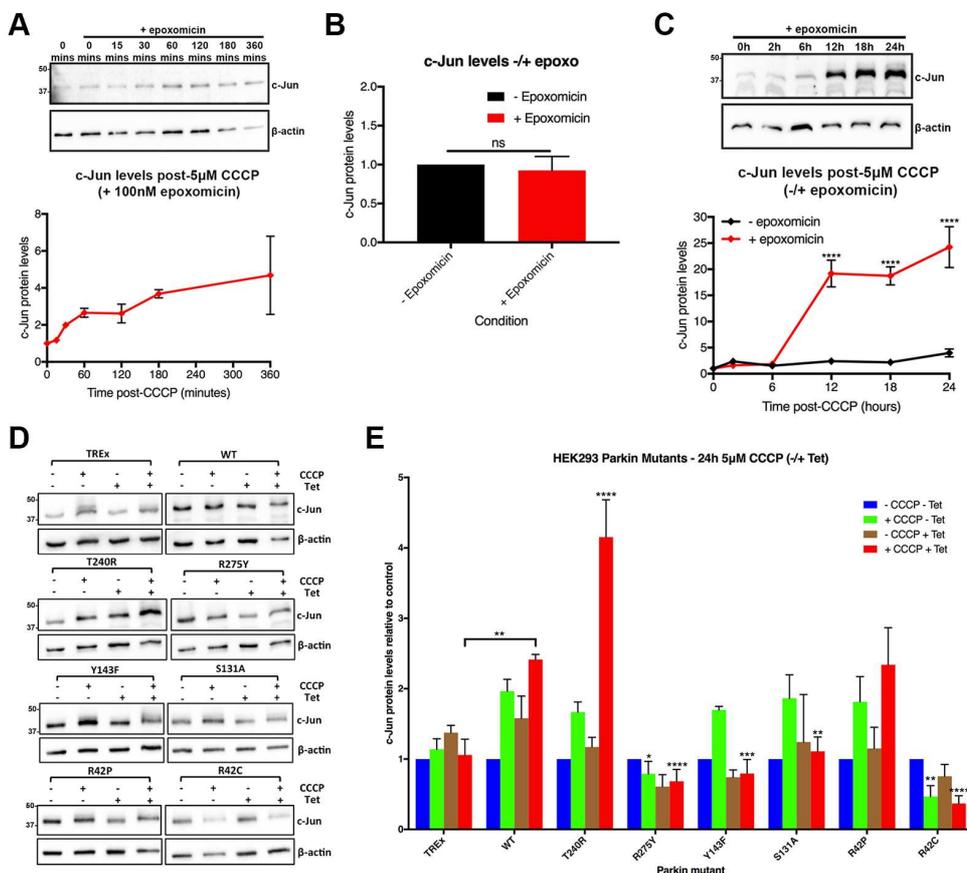
Figure 6: Parkin and c-Jun activity may be functionally linked. (A) Undifferentiated WT SH-SY5Y cells were treated with 100nM epoxomicin 1h prior to challenge with 5µM CCCP for up to 6h. Extracts were obtained at required time points for analysis by western blotting and c-Jun levels were calculated relative to b-actin. (*n* = 3). (B) Densitometric analysis of western blots showed c-Jun levels relative to b-actin were comparable with and without 1 hour 100nM epoxomicin treatment in the absence of CCCP (*n* = 3). (C) Over a 24h period of uncoupling following proteasomal inhibition, a massive increase in c-Jun levels was observed from 6h onwards compared to cells undergoing uncoupling without epoxomicin treatment (*n* = 3). (D) In a HEK293 model, expression of different Parkin constructs was induced by tetracycline for 24h. Cells were then treated with 5mM CCCP for 24h and protein extracts used to measure c-Jun levels by western blotting. Representative western blots for each Parkin mutant are shown. (F) Quantitative densitometric analysis of these blots was performed (*n* = 3). c-Jun levels were compared to those in cells not treated with CCCP or tetracycline for each Parkin construct unless otherwise shown. T240R appears to exacerbate the c-Jun response. Statistical significance was ascertained by 2-way ANOVA (Bonferonni's) (*p<0.05, **p<0.01, ***p<0.005, ****p<0.001). Error bars represent SEM.
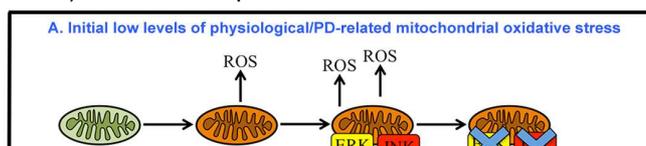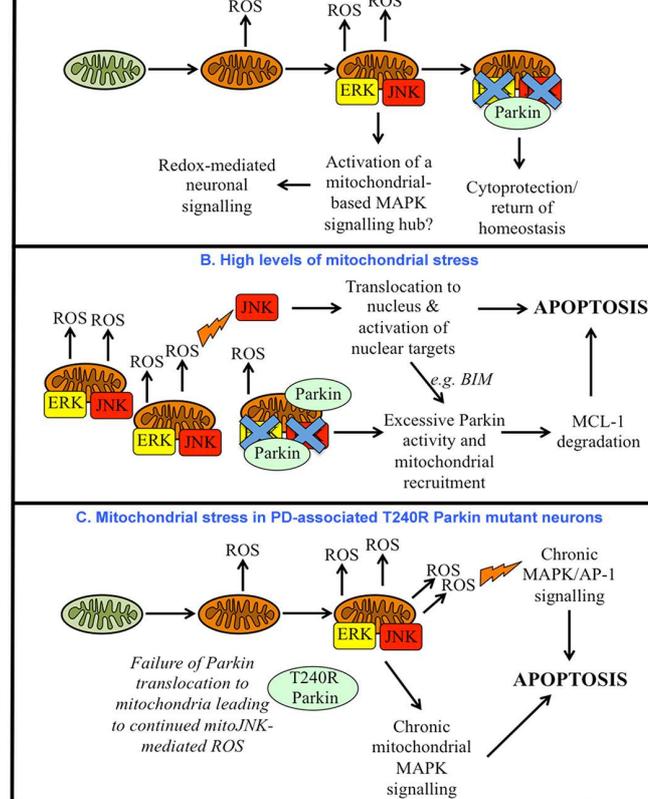
Figure 7: Potential regulatory pathways in the neuronal response to mitochondrial damage in PD. (A) Increased ROS production occurs in damaged mitochondria. Acute bursts of mitochondrial ROS initiate redox-sensitive signalling as part of normal neuronal function, with Parkin suppressing mitochondrial MAPK activity. Under these physiological conditions where, unlike models using uncouplers to induce mitochondrial damage in order to exaggerate *in vivo* situations, Parkin is cytoprotective. (B) High levels of stress activates MAPK signalling, RO accumulation and Parkin-dependent degradation of MCL-1. This leads to JNK/c-Jun pathways inducing the expression of pro-apoptotic genes such as *BIM*. Models using Parkin overexpression models will, however, lower the threshold at which Parkin promotes apoptosis under uncoupling conditions. (C) Some Parkin mutations antagonise its stress-induced mitochondrial translocation and resulting suppression of MAPK signalling. Mitochondrial ROS production increased by mitochondrial JNK activity promotes neuronal death pathways, which may be exacerbated by the failure of mutant Parkin to initiate mitophagy.

Supplementary information
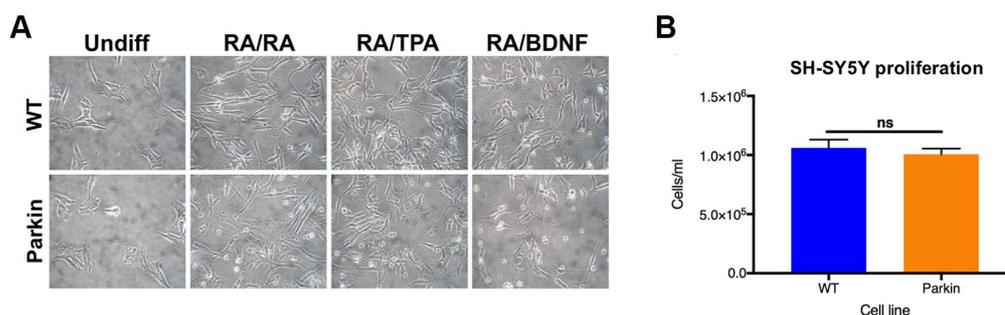
Figure S1: Differentiation and Parkin overexpression in SH-SY5Y cells. (A) Differentiation of SH-SY5Y cells using RA/BDNF resulted in greater observable neurite outgrowth relative to sequential treatment with RA (10% serum) then RA (0 % serum) (RA/RA) or RA (10% serum) then TPA (0.5% serum). Images were taken at 40X magnification to demonstrate morphological changes induced by the 3 methods. (C) Parkin expression does not affect the proliferation of SH-SY5Y cells (n = 3). Cells were plated at 100,000 cells/ml (2ml/well) and incubated for 72 hours before counting. Counts were analysed using an unpaired two-tailed *t*-test. Error bars represent SEM.
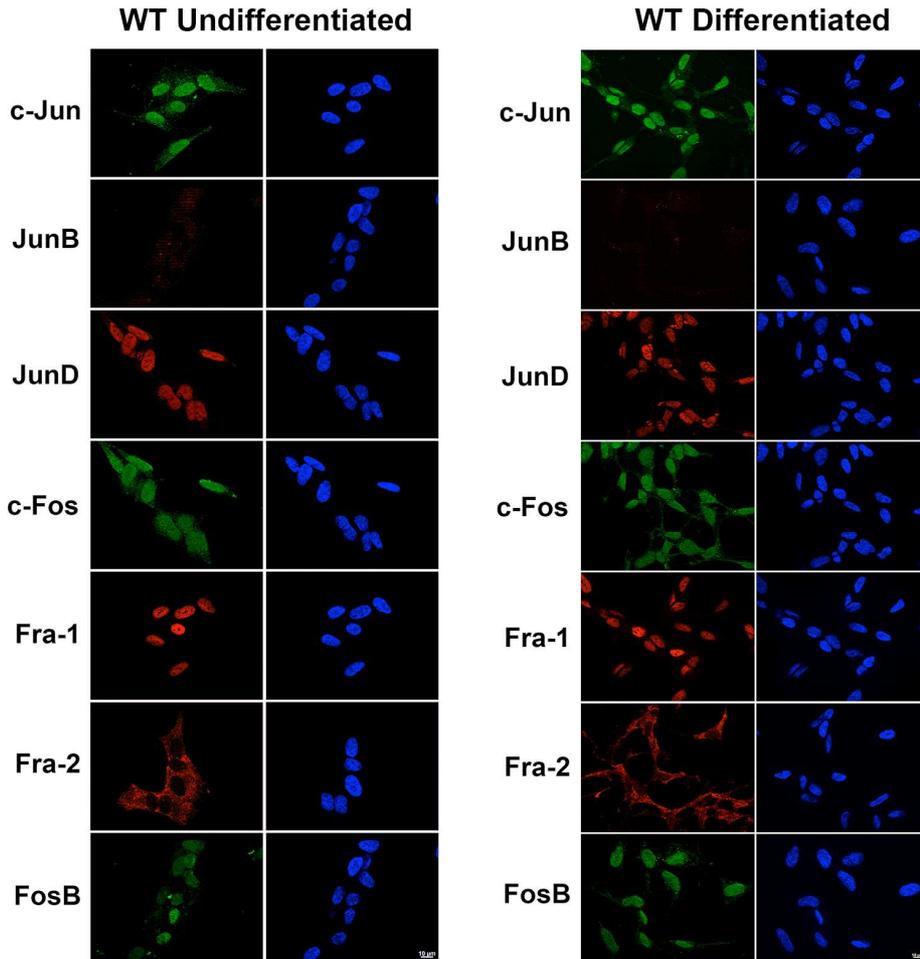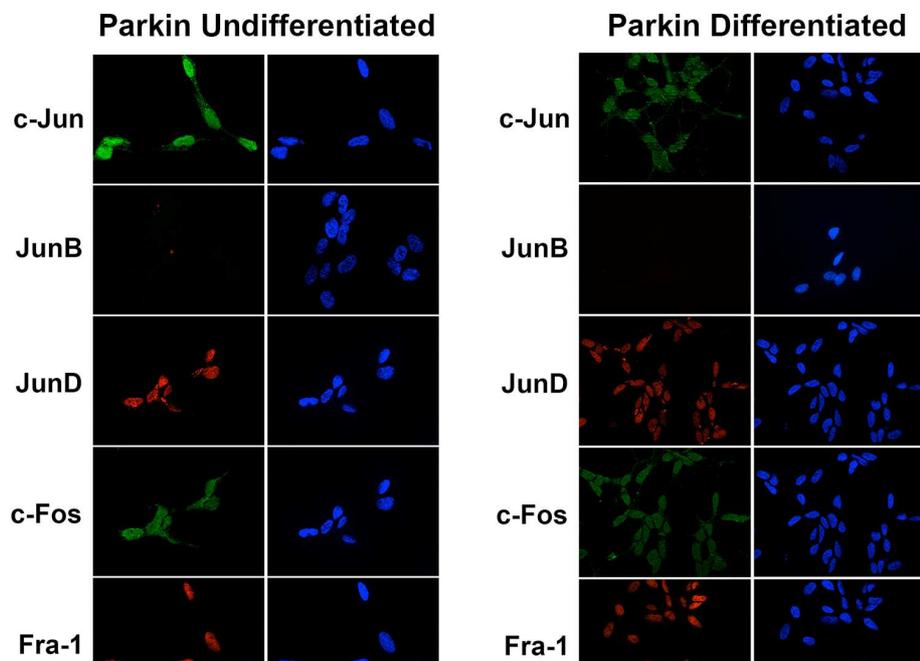
Figure S2: Immunofluorescence imaging of AP-1 proteins in WT SH-SY5Y cells. Cell nuclei were stained with DAPI (blue) and AP-1 proteins visualised as red or green. Images were captured at 100X magnification using a Zeiss Imager Z1 fluorescent microscope coupled to AxioVision software (scale bar – 10μm).
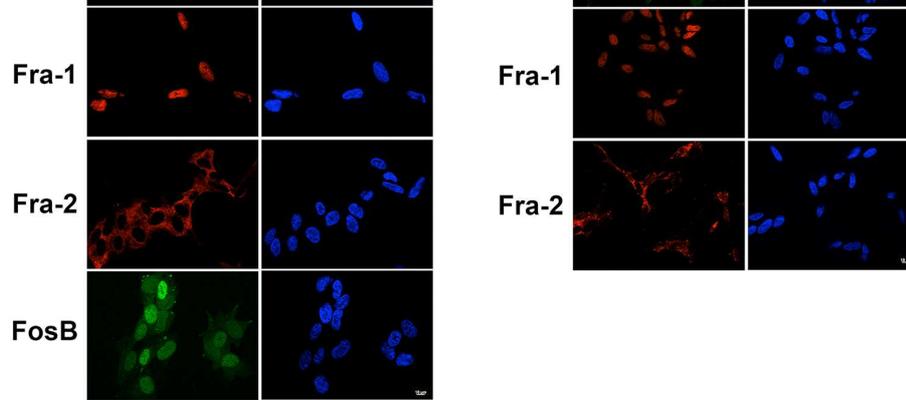
Figure S3: Immunofluorescence imaging of AP-1 proteins in Parkin overexpressing SH-SY5Y cells. Cell nuclei were stained with DAPI (blue) and AP-1 proteins visualised as red or green. Analysis of JunB by this method was not successfully performed and the experiment was not repeated. Images were captured at 100X magnification using a Zeiss Imager Z1 fluorescent microscope coupled to AxioVision software (scale bar – 10µm).
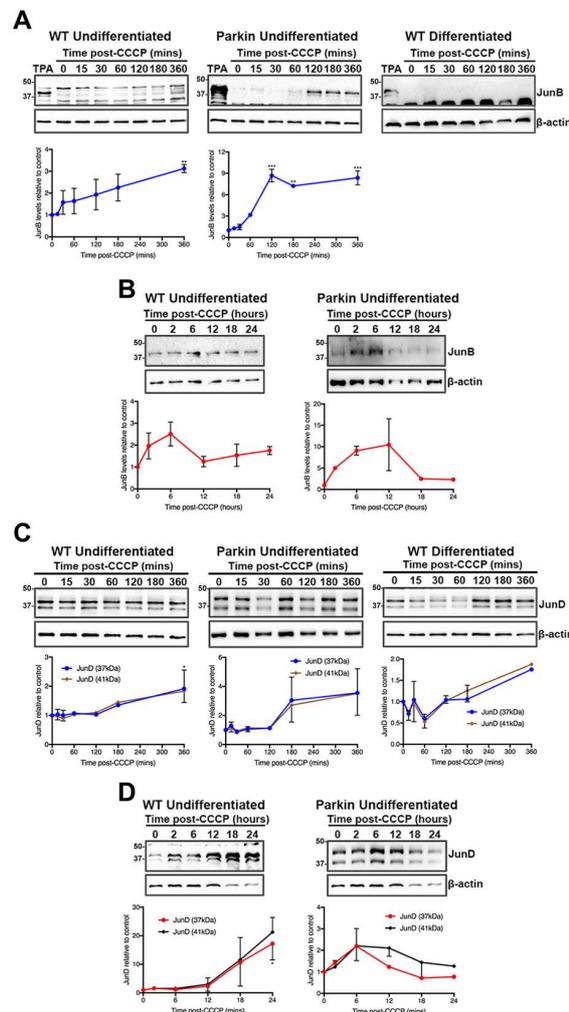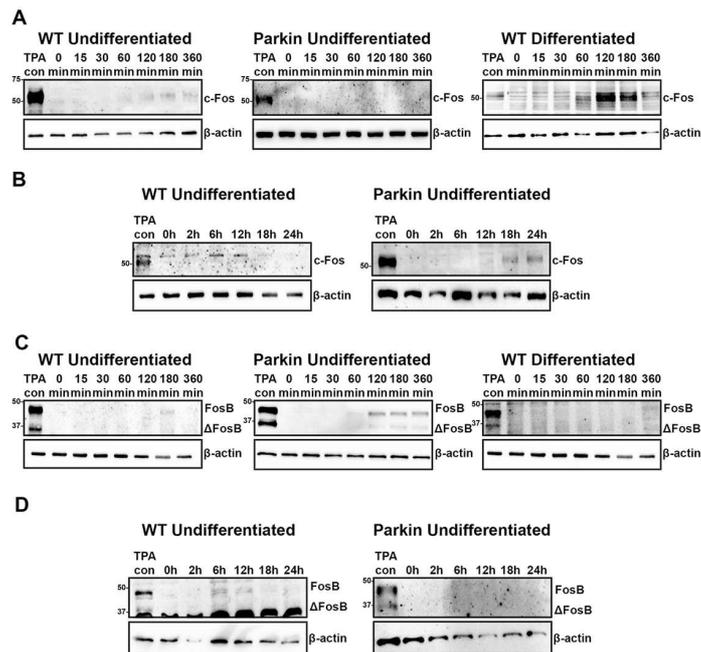

Figure S4: Modulation of JunB and JunD levels in response to mitochondrial uncoupling. Western blot analysis was carried out on protein extracts obtained at time points after the treatment of undifferentiated/differentiated WT or undifferentiated Parkin overexpressing SH-SY5Y cells with 5mM CCCP over 6 and 24h periods (*n* = 2). Differentiated cells were more sensitive to CCCP challenge so a sufficient quantity of extract was not obtained for the 24h assay. Densitometry was calculated relative to the loading control. (A) In comparison to WT undifferentiated cells, JunB underwent a more significant and rapid early increase in levels in Parkin overexpressing cells. No induction was detected in differentiated cells. TPA induction of JunB was used to confirm the analysis of the correct band. (B) In WT undifferentiated cells JunB levels peaked at 6h after uncoupling before decreasing then slowly increasing again to 24h. Parkin overexpression resulted in a greater increase before levels subsided. (C) The 37kDa (blue) and 41kDa (brown) JunD isoforms showed similar modulation in response to mitochondrial stress. (D) Parkin overexpression may repress the later elevation in JunD levels. Statistical significance was determined using a

decreasing then slowly increasing again to 2h. Parkin overexpression resulted in a greater increase before levels subsided. (C) The 37kDa (blue) and 41kDa (brown) JunD isoforms showed similar modulation in response to mitochondrial stress. (D) Parkin overexpression may repress the later elevation in JunD levels. Statistical significance was determined using a 2way ANOVA (Dunnett's) (*$p<0.05$, **$p<0.01$, ***$p<0.005$). Quantified levels were compared to levels at time point 0. Error bars represent SEM (37kDa – above, 41kDa – below).

Figure S5: c-Fos and FosB levels increase in response to mitochondrial uncoupling. Western blot analysis was carried out on protein extracts obtained at time points after the treatment of undifferentiated/differentiated WT or undifferentiated Parkin overexpressing SH-SY5Y cells with 5mM CCCP over a 6 or 24h period (*n* = 2). Differentiated cells were highly sensitive to CCCP challenge so c-Fos and FosB levels were not assessed for this cell line over 24h. Densitometry was not performed because proteins were undetectable under basal conditions. Cells treated with 100mg/ml TPA for 2h were used as a positive control. (A) Increased c-Fos levels peaking at 3h after uncoupling were detected in undifferentiated and differentiated WT cells, with higher levels being present in the latter. No increase was detected in undifferentiated Parkin overexpressing cells. (B) c-Fos levels peaked between 6-12h after uncoupling in WT undifferentiated cells before subsiding. In Parkin overexpressing cells increased levels were not seen until 18h post-uncoupling. (C) No early increase in levels of either FosB isoform was seen in WT cells. Parkin overexpression in undifferentiated cells resulted in increased levels of both FosB and DFosB by 2h after uncoupling. (D) FosB and DFosB protein was detected between 6-12h post- uncoupling in WT cells. No protein was detected in Parkin overexpressing cells, despite having been detected in the 6h assay. A non-specific band of a molecular weight below DFosB was observed in the WT extracts at all time points.
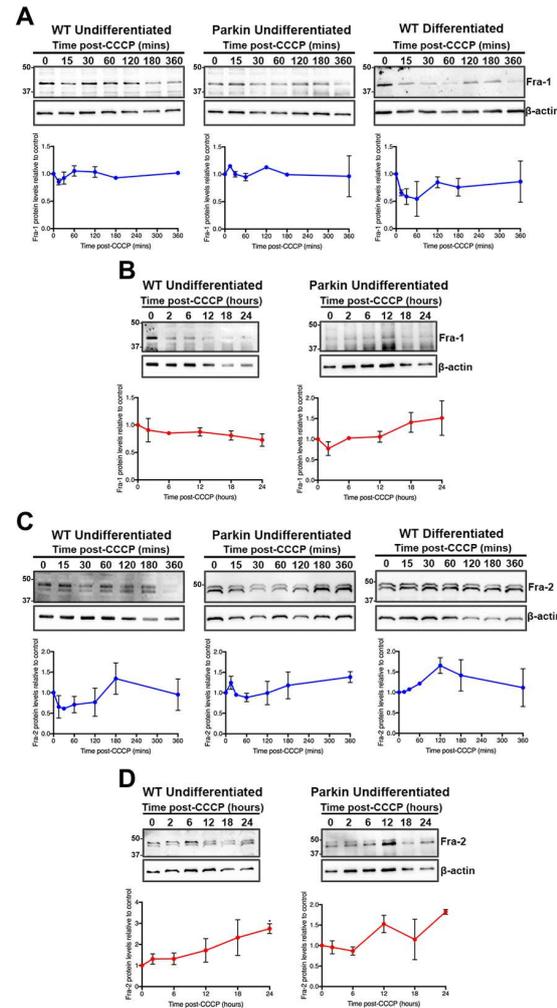
detected in Parkin overexpressing cells, despite having been detected in the 6h assay. A non-specific band of a molecular weight below ΔFosB was observed in the WT extracts at all time points.

Figure S6: Fra-1 and Fra-2 undergo regulation in response to CCCP. Western blot analysis was carried out on protein extracts obtained at time points after the treatment of undifferentiated/differentiated WT or undifferentiated Parkin overexpressing SH-SY5Y cells with 5mM CCCP over 6 and 24h periods (*n* = 2). Differentiated cells were highly sensitive to CCCP challenge so a sufficient quantity of extract was not obtained for the 24h assay. Densitometry was calculated relative to the loading control. (A) Fra-1 protein levels remained relatively constant over the first 6h of uncoupling in all cells examined. (B) A minor decrease or increase in Fra-1 levels occurred by 24h after uncoupling in WT and Parkin overexpressing cells respectively. (C) Only minor modulations of Fra-2 levels were seen in all cells after 6h uncoupling. (D) Fra-2 levels showed a general increase in undifferentiated WT and Parkin overexpressing cells over 24h of uncoupling. Statistical significance was determined using a 2way ANOVA (Dunnett's) (*p<0.05). Quantified levels were compared to levels at time point 0. Error bars represent SEM.
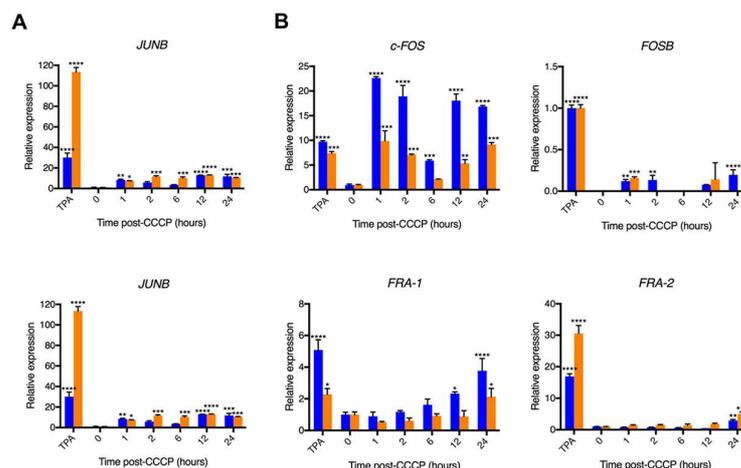

Figure S7: Modulation of AP-1 gene expression after mitochondrial uncoupling. cDNA obtained from RNA extracts over the 24h after 5mM CCCP challenge in undifferentiated WT SH-SY5Y cells was analysed for relative expression of the individual AP-1 genes by qPCR. Expression levels were relative to the 0h time point and were the mean totals (A) *JUNB* and

Figure S7: Modulation of AP-1 gene expression after mitochondrial uncoupling. cDNA obtained from RNA extracts over the 24h after 5mM CCCP challenge in undifferentiated WT SH-SY5Y cells was analysed for relative expression of the individual AP-1 genes by qPCR. Expression levels are relative to the 0h time point, unless otherwise stated. (A) *JUNB and JUND* expression in response to CCCP challenge show these genes are induced. (B) *c-FOS* and *FOSB* were modulated more rapidly than *FRA-1* and *FRA-2* and also showed a biphasic response that was not observed in the latter. As *FOSB* mRNA was not detectable under basal conditions, values are relative to the TPA-induced control for this gene. Graphs show 2 independent biological replicates (1st – blue, 2nd – orange) (*n* = 2). Statistical significance was determined using a 2way ANOVA (Dunnett's) (*$p<0.05$, **$p<0.01$, ***$p<0.005$, ****$p<0.001$). Quantified levels were compared to levels at time point 0 unless otherwise stated by horizontal bars. Error bars represent SD.
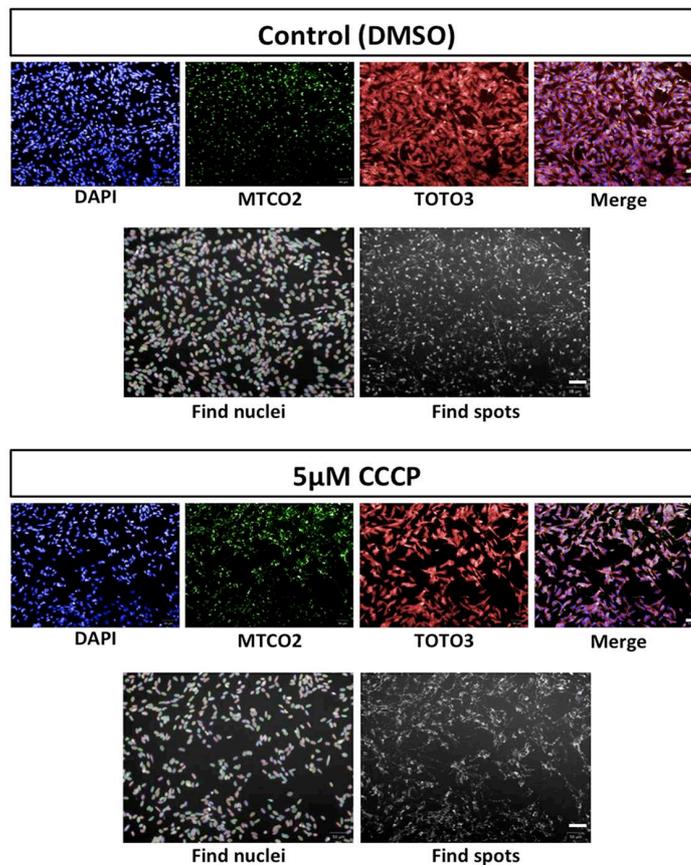

Figure S8: An example of Columbus software analysis of images captured using the Operetta system. Images were captured using the 20X lens. Nuclei (DAPI – blue), mitochondria (MTCO2 – green) and cytoplasm (TOTO-3 – red) were labelled for imaging. Columbus software then calculated the number of mitochondrial 'spots' or 'clusters' (FITC channel) per cell (DAPI channel) for every well. Scale bars for both image sizes are 50µM.

28